

Journal Pre-proofs

Synthesis, α -glucosidase inhibition and antioxidant activity of the 7-carbo-substituted 5-bromo-3-methylindazoles

Malose J. Mphahlele, Nontokozo M. Magwaza, Samantha Gildenhuis, Itumeleng B. Setshedi

PII: S0045-2068(19)32217-5
DOI: <https://doi.org/10.1016/j.bioorg.2020.103702>
Reference: YBIOO 103702

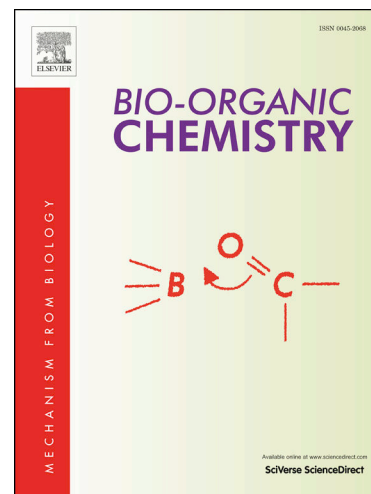
To appear in: *Bioorganic Chemistry*

Received Date: 25 December 2019
Revised Date: 23 February 2020
Accepted Date: 24 February 2020

Please cite this article as: M.J. Mphahlele, N.M. Magwaza, S. Gildenhuis, I.B. Setshedi, Synthesis, α -glucosidase inhibition and antioxidant activity of the 7-carbo-substituted 5-bromo-3-methylindazoles, *Bioorganic Chemistry* (2020), doi: <https://doi.org/10.1016/j.bioorg.2020.103702>

This is a PDF file of an article that has undergone enhancements after acceptance, such as the addition of a cover page and metadata, and formatting for readability, but it is not yet the definitive version of record. This version will undergo additional copyediting, typesetting and review before it is published in its final form, but we are providing this version to give early visibility of the article. Please note that, during the production process, errors may be discovered which could affect the content, and all legal disclaimers that apply to the journal pertain.

© 2020 Published by Elsevier Inc.



Synthesis, α -glucosidase inhibition and antioxidant activity of the 7-carbo-substituted 5-bromo-3-methylindazoles

Malose J. Mphahlele,^{1*} Nontokozo M. Magwaza,¹ Samantha Gildenhuis² and Itumeleng B. Setshedi²

¹ Department of Chemistry, College of Science, Engineering and Technology, University of South Africa, Private Bag X06, Florida 1710, South Africa

² Department of Life & Consumer Sciences, College of Agriculture and Environmental Sciences, University of South Africa, Private Bag X06, Florida 1710, South Africa

*Author for correspondence; mphahmj@unisa.ac.za

Abstract: Series of 7-aryl- (**3a–f**), 7-arylvinyl- (**3g–k**) and 7-(arylethynyl)-5-bromo-3-methylindazoles (**4a–f**) have been evaluated through enzymatic assay *in vitro* for inhibitory effect against α -glucosidase activity and for antioxidant potential through the 2,2-diphenyl-1-picrylhydrazyl (DPPH) radical scavenging assay. Compounds **3a–k** and **4a–f** showed significant to moderate α -glucosidase inhibition with IC_{50} values in the range of 0.50–51.51 μ M and 0.42–23.71 μ M compared with acarbose drug ($IC_{50} = 0.82 \mu$ M), respectively. 5-Bromo-3-methyl-7-phenyl-1*H*-indazole (**3a**), 5-bromo-3-methyl-7-styryl-1*H*-indazole (**3h**) and 5-bromo-3-methyl-7-styryl-1*H*-indazole (**4a**) exhibited moderate to significant antigrowth effect against the breast MCF-7 cancer cell line and reduced cytotoxicity against the human embryonic kidney derived Hek293-T cells when compared to doxorubicin as reference standard. Non-covalent (alkyl, π -alkyl and π - π T shaped), electrostatic (π -sulfur and/or π -anion) and hydrogen bonding interactions are predicted to increase interactions with protein residues, thereby enhancing the inhibitory effect of these compounds against α -glucosidase.

Keywords: polysubstituted indazoles; α -glucosidase; antioxidant activity; cytotoxicity; molecular docking

1. Introduction

Type 2 diabetes (T2D) mellitus is a chronic non-communicable metabolic disease, and its prevalence has been rising steadily over the year to become a serious public health problem [1]. This disease is characterized by a defect in the secretion of insulin and resistance in its target organs. The deficiency is attributed to increased glucose level in blood, also known as post-prandial hyperglycemia (PPHG). PPHG has emerged as a prominent and early defect in type 2 diabetes [2]. Diabetic patients are more vulnerable to various forms of both short- and long-term complications, such as an increased risk of microbial infections [3] and cancer [4-6]. Hyperglycemia, has also been linked to increased cancer cell proliferation, inhibited cancer cell apoptosis and increased cancer cell metastasis [7]. α -Glucosidase is a membrane bound enzyme in small intestine responsible for inhibiting the hydrolysis of carbohydrates [8]. This enzyme catalyzes the hydrolysis of 1,4- α bonds of the unabsorbed oligo- and disaccharides, and converts them into glucose, which is absorbed in the upper jejunum resulting in hyperglycaemia [9]. Inhibitors of α -glucosidase can retard the decomposition and absorption of dietary carbohydrates by restricting the breakdown of linear or branched oligosaccharide units like α -limit dextrins, maltose and maltotriose to produce glucose, thereby preventing glucose absorption into blood stream and suppressing PPHG [10,11]. Oxidative stress is implicated in the early stages and progression of T2D due to the ability of free radicals to damage lipids, proteins and DNA [12]. Preclinical and clinical studies, on the other hand, have revealed complex associations between diabetes and breast cancer [7]. Inhibition of α -glucosidase has also been found to have positive effects in the treatment of cancer [13]. Managing diabetes and treating cancer using a combination of anti-diabetic, antioxidant and classical anti-cancer drugs has proven to be more efficient in the treatment of diabetes-associated cancers. Metformin (1,1-dimethylbiguanidehydrochloride), is the most widely used oral anti-diabetic drug for the treatment of diabetes and has also shown promise in reducing cancer risk with little or no

negative effects [14]. Thus, drugs that mitigate PPHG and possess cytotoxic activity against breast cancer may offer an opportunity for the development of novel therapeutics for diabetic patients. Such a multi-target-directed ligand design strategy (MTDL) would probably be more effective for the treatment of diabetes than one-target one-drug concepts and drug-combination therapies.

The indazole moiety is a 2-azaindole bioisoster, and it continues to attract considerable attention especially in the context of anti-diabetic [15-17] and anticancer [18,19] drug development. Hydrophobic interactions, including alkyl, π -alkyl and π - π interactions between inhibitors and α -glucosidase play a significant role in inhibitory activities of this enzyme [20]. Literature precedents revealed that a methyl group at the 3-position of the indazole ring is well tolerated with respect to anti-diabetic potency *in vitro* [15,17]. Song *et al.* prepared series of N-1 or N-2 substituted indazoles bearing an aryl group at either position 5 or 6, and with or without a carbon-based substituent at the C-3 position and evaluated them *in vitro* and *in vivo* as glucagon receptor antagonists [17]. The C-3 unsubstituted derivatives were found to be strongly active than the 3-methyl substituted derivatives, which in turn, were more active than the 3-aryl substituted analogues. The presence of bromine on the fused benzo ring of the 1*H*-indazole framework, on the other hand, has been found to increase the inhibitory activity against indoleamine 2,3-dioxygenase 1 (IDO1) activity [21]. Moreover, a bromine atom is known to contain a region with positive charge, which is responsible for this atom's directional and stabilizing characteristics on the drug molecules [22]. It was envisaged that a bromine atom and carbon-based substituents (methyl and aryl groups) on the 1*H*-indazole scaffold would increase hydrophobic interactions and result in increased inhibitory effect against α -glucosidase. With these assumptions in mind, series of 3-methyl-1*H*-indazoles substituted with a lipophilic bromine atom at the 5-position and an aryl ring linked at position-7 directly or via a π -conjugated spacer (C=C or C \equiv C) were synthesized for evaluation of biological activity as potential anti-diabetic agents. The 7-carbo-substituted 5-bromo-3-methyl-1*H*-indazoles have been prepared

via Suzuki-Miyaura cross-coupling of arylboronic and vinylboronic acids as well as Sonogashira cross-coupling with phenylacetylene derivatives. The compounds were evaluated via enzymatic assay *in vitro* for inhibitory effect against α -glucosidase activity and for antioxidant potential using the DPPH radical scavenging assay. The most active compounds against α -glucosidase were also evaluated for antigrowth effect against the breast MCF-7 cancer cell line and also for cytotoxicity against the Hek293-T cells. Representative compounds from each series were selected for a kinetic study and for molecular docking into the binding pocket of the aforementioned enzyme to determine plausible protein-ligand interactions on a molecular level.

2. Results and Discussion

2.1. Chemistry

The synthesis of the aforementioned compounds and their substitution patterns are represented in Scheme 1 and Table 1, respectively. First 2-amino-5-bromo-3-iodoacetophenone oxime (**1**) was subjected to methanesulfonyl chloride in the presence of trimethylamine in dichloromethane at room temperature (RT) for 4 h to afford upon aqueous work-up and column chromatography on silica gel 5-bromo-7-iodo-3-methylindazole (**2**). The analogous mixed dihalogenated indazoles substituted with iodine at the C-3 position and bromine at the 5 or 7 positions have previously been transformed into polycarbo-substituted indazoles via palladium catalyzed cross-coupling reactions [23]. Compound **2** was subjected to Suzuki-Miyaura cross-coupling with various arylboronic and arylvinylboronic acids in the presence of dichlorobis(triphenylphosphine)palladium(II) ($\text{PdCl}_2(\text{PPh}_3)_2$) as a source of active Pd(0) species and potassium carbonate as a base in 4:1 toluene-ethanol (v/v) at 80 °C under reflux for 18 h. Aqueous work-up and purification by silica gel column chromatography afforded the corresponding 7-aryl- **3a–g** and arylvinyl substituted indazoles **3h–k** (Scheme 1). The ^1H NMR

and ^{13}C NMR spectra of compounds **3a–k** showed increased number of peaks in the aromatic region. The ^1H NMR spectra of **3h–k** revealed additional set of doublets in the aromatic region with coupling constant values $J = 16.0$ Hz typical for the *trans* vinyl moiety. Sonogashira cross-coupling of compound **1** with terminal acetylenes in the presence of $\text{PdCl}_2(\text{PPh}_3)_2$ -copper iodide catalyst mixture and cesium carbonate in aqueous tetrahydrofuran (THF) at room temperature (RT) afforded after 3 h by aqueous work-up and purification by column chromatography on silica gel, the homocoupled dimer and a single cross-coupled product **4a–f**. The ^1H NMR and ^{13}C NMR spectra of the 7-arylethynyl substituted 5-bromo-3-methylindazoles **4a–f** showed increased number of peaks in the aromatic region confirming the formation of the cross-coupled product. The alkynyl nature of compounds **4a–f** was confirmed by the presence of additional set of singlets in the region δ 83.0–86.0 ppm and δ 93.0–96.0 ppm corresponding to the carbon atoms of the triple bond. Exclusive substitution at the $\text{Csp}^2\text{–I}$ bond was confirmed in the molecular ion region of the mass spectra of compounds **3** and **4** of M^+ and $\text{M}+2$ in the ratio 1:1 due to the presence of the ^{79}Br and ^{81}Br isotopes in the molecular ions. The 7-phenyl- and 7-styryl- substituted derivatives **3a** and **3h** were formed in comparable yield, 65% and 67%, respectively. A similar trend was observed for the Suzuki-Miyaura cross-coupling of **2** to afford 7-(4-methoxyphenyl)- **3e** and the 7-(4-methoxystyryl)- derivative **3k** in 52% and 50% yield, respectively. Moderate yields were observed for the 7-(4-fluorostyryl)- and 7-(4-chlorostyryl)- substituted derivatives **3i** (56%) and **3j** (54%) when compared to the corresponding 7-(4-fluorophenyl)- and 7-(4-chlorophenyl)- substituted analogues **3b** (81%) and **3c** (66%), respectively. Compound **3e** substituted with a strongly electron withdrawing trifluoromethoxy group at the *para* position of the phenyl ring and **3g** substituted with a combination of strongly electronegative 3-chloro and 4-fluoro atoms on the phenyl ring were isolated in 50% and 52% yield, respectively. However, relatively high yield (64%) was observed for **3f** substituted with a strongly electron-withdrawing aminocarbonyl group on the *meta* position of the phenyl ring. The presence of 3-(fluorophenyl)ethynyl- or 3-(chlorophenyl)ethynyl- group at the 7-position

of the indazole scaffold of **3b** or **3d** resulted in relatively higher yield (76% and 72%, respectively) than the isomeric 4-(halogenophenyl)ethynyl derivatives **4c** (64%) and **4e** (69%). Increased yield was observed for **4f** (78%) bearing a strongly electron delocalizing methoxy group at the *para* position of the phenylethynyl moiety.

Scheme 1: Suzuki-Miyaura and Sonogashira cross-coupling of **2** to afford **3a–k** and **4a–f**, respectively.

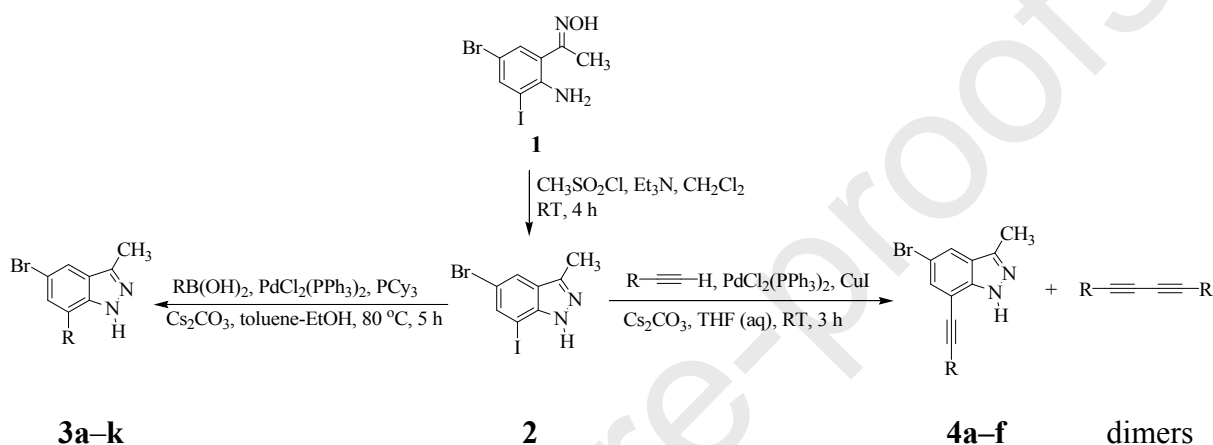


Table 1: Substitution patterns of compounds **3a–k** and **4a–f**.

3: R =	C ₆ H ₅ - (3a); 4-FC ₆ H ₄ - (3b); 4-ClC ₆ H ₄ - (3c); 4-MeOC ₆ H ₄ - (3d); 4-CF ₃ OC ₆ H ₄ - (3e); 3-NH ₂ C(O)C ₆ H ₄ - (3f); 3-Cl,4-FC ₆ H ₃ - (3g); C ₆ H ₅ CH=CH- (3h); 4-FC ₆ H ₄ CH=CH- (3i); 4-ClC ₆ H ₄ CH=CH- (3j); 4-CH ₃ OC ₆ H ₄ CH=CH- (3k)
4: R =	C ₆ H ₅ - (4a); 3-FC ₆ H ₄ - (4b); 4-FC ₆ H ₄ - (4c); 3-ClC ₆ H ₄ - (4d); 4-ClC ₆ H ₄ - (4e); 4-MeOC ₆ H ₄ - (4f)

2.2. Biological evaluation of compounds **2**, **3a–k** and **4a–f**.

Compounds **2**, **3a–k** and **4a–f** were evaluated for inhibitory effect *in vitro* through enzymatic assays against α -glucosidase activity to correlate between both structural variations and biological activity. Since free radical-mediated oxidative stress is also implicated in the early stages of T2D and cancer [24], these compounds were evaluated for antioxidant activity in the DPPH radical scavenging assay. Moreover, the most active compounds against α -

glucosidase were also evaluated for potential cytotoxicity against the breast MCF-7 cancer cell line and the normal Hek293-T cells. Structure activity relationship has been rationalized in terms of substitution pattern on the phenyl group and its connectivity to the 7-position of the indazole framework.

2.2.1. α -Glucosidase inhibitory activity and antioxidant potential of **2**, **3a–k** and **4a–f**

The inhibitory activities of compounds **2**, **3a–k** and **4a–f** against α -glucosidase were evaluated using the *Saccharomyces cerevisiae* form of enzyme against acarbose, a well-known inhibitor of α -glucosidase [8]. The results are expressed as IC_{50} values, i.e., the concentration of each sample required inhibit 50% of the α -glucosidase activity (Table 2). 5-Bromo-7-iodo-3-methylindazole (**2**) was found to be less active against this enzyme when compared to the reference standard acarbose ($IC_{50} = 0.82 \mu\text{M}$) with an IC_{50} value of $11.69 \mu\text{M}$. The three series of 7-carbo substituted derivatives exhibited variable degree of activity with IC_{50} values ranging from 0.42 to $51.50 \mu\text{M}$ when compared with the standard acarbose having IC_{50} value $0.82 \mu\text{M}$. Replacement of iodine with a phenyl group resulted in increased inhibitory effect for **3a** against α -glucosidase with an IC_{50} value of $0.53 \mu\text{M}$. Except for the 7-(4-trifluoromethoxyphenyl) substituted derivative **3e** with an IC_{50} value of $0.75 \mu\text{M}$, derivatives **3b–d** and **3f** substituted at the *para* position of the 7-phenyl ring with an electron donating ($-\text{OCH}_3$) or withdrawing (F, Cl or $\text{NH}_2\text{C}(\text{O})-$) group were found to be less active against this enzyme. The observed increased activity for compound **3e** is probably due to the presence of the trifluoromethoxy ($-\text{OCF}_3$) group, which is both more electron withdrawing and lipophilic than its methoxy analogue and also far more lipophilic than the halogen atoms [25]. This group has previously been found to increase biological activity of the molecule due to its enhanced lipid solubility and metabolic stability [25]. Moreover, the strong electron-withdrawing effect of the halogen atoms helps in forming halogen and/or hydrogen bonds that help to increase the number of interactions of drug molecules with their protein targets, thereby enhancing biological activity [26]. The presence of 3-chloro-4-fluorophenyl group on the indazole scaffold of **3g** resulted in moderate inhibitory

activity for this compound with an IC_{50} value of 5.49 μM . The presence of the carbon–carbon double bond linker in the series **3h–k** resulted in slightly increased inhibitory effect for the 7-styryl substituted derivative **3h** ($IC_{50} = 0.50 \mu\text{M}$) than **3a** ($IC_{50} = 0.53 \mu\text{M}$) in which the phenyl substituent is linked directly to the fused benzo ring of the indazole scaffold. The 4-fluorophenylstyryl substituted derivative **3i** behaved like the 4-fluorophenyl substituted derivative **3b** and both compounds were found to be less active against this enzyme with IC_{50} values of 51.51 μM and $IC_{50} = 51.07 \mu\text{M}$, respectively. The presence of the carbon–carbon double bond linker between the indazole scaffold and 4-chlorophenyl group resulted in moderate inhibitory effect of **3j** ($IC_{50} = 7.73 \mu\text{M}$) when compared to the 4-chlorophenyl substituted analogue **3c** ($IC_{50} = 22.68 \mu\text{M}$). The presence of the more polar lipophilic methoxystyryl ($R = 4-(\text{CH}_3\text{OC}_6\text{H}_4)\text{CH}=\text{CH}-$) group in compound **3k** resulted in increased inhibitory effect for this compound with an IC_{50} value of 0.80 μM , which is comparable to that of acarbose ($IC_{50} = 0.82 \mu\text{M}$). The presence of a carbon-carbon triple bond between the indazole scaffold and aryl group resulted in variable degree of activity within the series **4a–f**. The parent compound **4a** was found to be the most active within this series and among all the compounds tested with an IC_{50} value of 0.43 μM . The presence of a $-\text{C}\equiv\text{C}-$ bridge also resulted in significant inhibitory activity for the 3- and 4-halogenophenyl substituted derivatives **4b**, **4c**, **4d** and **4e** against α -glucosidase with IC_{50} values 7.14, 5.27, 3.42 and 4.87 μM , respectively. However, loss of activity was observed for compound **4f** with a carbon–carbon triple bond linker between the indazole scaffold and the 7-(4-methoxyphenyl) group. Within the three series of compounds, derivatives in which the phenyl ring is linked to the 7-position of the indazole scaffold directly (**3a**: $R = \text{C}_6\text{H}_5-$) or *via* a π -conjugated spacer, viz., $\text{C}=\text{C}$ (**3h**: $R = \text{C}_6\text{H}_5\text{CH}=\text{CH}-$) or) or $\text{C}\equiv\text{C}$ (**4a**: $R = \text{C}_6\text{H}_5\text{C}\equiv\text{C}-$) bond have been found to exhibit increased inhibitory effect against α -glucosidase and the trend is as follows: **4a** ($IC_{50} = 0.42 \mu\text{M}$) > **3h** ($IC_{50} = 0.50 \mu\text{M}$) > **3a** ($IC_{50} = 0.53 \mu\text{M}$).

Famuyiwa *et al.* have recently demonstrated the link between anti-diabetic and antioxidant activities of drugs through *in vivo* experiments and theoretical calculations using protocatechuic

acid and glibenclamide as models [27]. Increased reactive oxygen species (ROS) production in the liver and adipose tissue of high fat diet-fed mice has been found to be linked with insulin resistance [28], and this effect was reversed by the use of antioxidants [29]. Indazole and its derivatives were previously found to significantly inhibit 2,2-diphenyl-1-picrylhydrazyl (DPPH) free radical generation in a concentration dependent manner [30]. This literature precedent encouraged us to evaluate compounds **2**, **3a–k** and **4a–f** for free radical scavenging activity *in vitro* using the DPPH free-radical scavenging method (Table 2). The natural antioxidants ascorbic acid was used as a positive control [31]. Compound **2** was found to exhibit significant antioxidant effect when compared to ascorbic acid ($IC_{50} = 5.20 \mu\text{M}$) with an IC_{50} value of $6.79 \mu\text{M}$. Compound **3a** which is one the highest active derivatives against α -glucosidase ($IC_{50} = 0.53 \mu\text{M}$) within the series **3a–k** also exhibited increased free radical scavenging activity with an IC_{50} value of $4.99 \mu\text{M}$. The 7-(4-fluorophenyl) substituted derivative **3b** ($IC_{50} = 50.52 \mu\text{M}$) was found to exhibit reduced antioxidant properties when compared to the 7-(4-chlorophenyl) analogue **3c** ($IC_{50} = 0.91 \mu\text{M}$). No antioxidant activity was observed for the 4-methoxyphenyl substituted derivative **3d** ($IC_{50} = 49.40 \mu\text{M}$) whereas the analogous 7-(4-trifluoromethylphenyl) analogue **3e** exhibited increased antioxidant activity when ($IC_{50} = 4.84 \mu\text{M}$) when compared to the reference standard. Compound **3f** also exhibited reduced antioxidant activity with an IC_{50} value of $26.33 \mu\text{M}$. A combination of 3-chloro and 4-fluoro atoms on the phenyl substituent of **3g** resulted in increased antioxidant activity for this compound ($IC_{50} = 4.62 \mu\text{M}$). The presence of a carbon-carbon double bond bridge between the phenyl ring and the indazole scaffold resulted in significant antioxidant effect for **3h** ($IC_{50} = 7.10 \mu\text{M}$) though less when compared to **3a** ($IC_{50} = 4.99 \mu\text{M}$) in which the phenyl ring is linked directly to the heterocyclic framework. Compounds **3i** and **3k** substituted with moderately and strongly electron delocalizing 4-fluorophenyl or 4-methoxyphenyl groups at position-7 were found to exhibit moderate antioxidant activity with IC_{50} values $15.30 \mu\text{M}$ and $14.46 \mu\text{M}$, respectively. The 2-chlorostyryl derivative **3j** was found to be the most active

within the styryl substituted series **3j–k**, more so than ascorbic acid with an IC_{50} value of 1.06 μ M. The presence of a carbon-carbon triple bond linker between the phenyl ring and the indazole scaffold resulted in significantly increased antioxidant activity for **4a** ($IC_{50} = 1.00 \mu$ M). The presence of a halogen atom on the *meta* position of the 7-phenyl ring resulted in reduced antioxidant activities for compounds **4b** and **4d** with IC_{50} values of 88.66 μ M and 66.20 μ M, respectively. However, significant antioxidant activity was observed for the isomeric 7-(4-fluorophenyl) substituted derivative **4c** with an IC_{50} value of 7.96 μ M. The presence of the strongly electron delocalizing 4-methoxyphenyl group at the 7-position of the indazole framework, on the other hand, resulted in increased antioxidant activity for **4f** with an IC_{50} value of 4.92 μ M. Compounds **3a**, **3e**, **3h** and **4a** exhibit dual anti- α -glucosidase and antioxidant properties. Though strongly inhibiting against α -glucosidase, compound **3k** was found to exhibit moderate antioxidant effect when compared to ascorbic acid with an IC_{50} value of 14.46 μ M.

Literature survey revealed several studies highlighting the fact that T2D is a risk factor for cancer, with some oral hypoglycemic drugs such as metformin therapy associated with a significant reduction in cancer incidence, especially gastrointestinal and breast cancers. Since breast cancer is related to T2D [7], the most active compounds against α -glucosidase, namely, **3a**, **3e**, **3h**, **3k** and **4a** were also screened for antigrowth effects *in vitro* against the breast MCF-7 cancer cell line using the 3-(4,5-dimethylthiazol-2-yl)-2,5-diphenyltetrazolium bromide (MTT) tetrazolium reduction assay. Doxorubicin (Doxo) was used as a positive control for this assay because this drug was previously found to inhibit MCF-7 cell proliferation [32]. The preliminary results of this assay revealed compound **3a**, **3h** and **4a** to exhibit moderate to significant cytotoxicity against this cell line when compared to Doxo ($IC_{50} = 36.03 \mu$ M) and the trend is as follows: **4a** ($IC_{50} = 35.13 \mu$ M) > **3h** ($IC_{50} = 39.33 \mu$ M) > **3a** ($IC_{50} = 49.90 \mu$ M). These compounds were also evaluated for toxicity against the human embryonic kidney (Hek293-T) cell line using the clinical drug Doxo as reference standard. The IC_{50} values of **3a**,

3e, **3h**, **3k** and **4a** against the normal Hek293-T cells were found to be $19.01 \pm 0.14 \mu\text{g/mL}$, $23.01 \pm 0.22 \mu\text{g/mL}$, $24.00 \pm 0.18 \mu\text{g/mL}$, $25.01 \pm 0.15 \mu\text{g/mL}$ and $18.03 \pm 0.09 \mu\text{g/mL}$, respectively, as compared to the clinical drug, doxorubicin ($\text{IC}_{50} = 5.02 \pm 0.07 \mu\text{g/mL}$). The non-cancer-derived Hek293-T cell line has been found to be highly sensitivity to free Doxo [33]. Compounds **3a**, **3e**, **3h**, **3k** and **4a** exhibited reduced cytotoxicity against Hek293-T cells, which suggests good cytocompatibility for the test compounds.

Table 2: α -Glucosidase inhibitory and antioxidant activities of **2–4**, and cytotoxicity against **3a**, **3e**, **3h**, **3k** and **4a**.

2–4	IC ₅₀ values (μM)		
	α -Glucosidase	DPPH	MCF-7 (*SI)
2	11.69 ± 0.010	6.79 ± 0.003	-
3a	0.53 ± 0.013	4.99 ± 0.006	49.90 ± 0.02 (2.62)
3b	51.07 ± 0.001	50.52 ± 0.001	-
3c	22.68 ± 0.001	0.91 ± 0.004	-
3d	13.52 ± 0.006	49.40 ± 0.003	-
3e	0.75 ± 0.006	4.84 ± 0.009	71.94 ± 0.05 (3.12)
3f	22.7 ± 0.012	26.33 ± 0.005	-
3g	5.49 ± 0.003	4.62 ± 0.005	-
3h	0.50 ± 0.010	7.10 ± 0.004	39.33 ± 0.02 (1.64)
3i	51.51 ± 0.013	15.30 ± 0.003	-
3j	7.73 ± 0.004	1.06 ± 0.013	-
3k	0.80 ± 0.009	14.46 ± 0.009	53.25 ± 0.05 (2.13)
4a	0.42 ± 0.019	1.00 ± 0.007	35.13 ± 0.02 (1.95)
4b	7.14 ± 0.009	88.66 ± 0.001	-
4c	5.27 ± 0.004	7.96 ± 0.001	-

4d	3.42 ± 0.002	66.20 ± 0.01	-
4e	4.87 ± 0.004	27.83 ± 0.01	-
4f	23.71 ± 0.004	4.92 ± 0.01	-
Acarbose	0.82 ± 0.006	-	-
Ascorbic acid	-	5.20 ± 0.006	-
Doxorubicin	-	-	36.03 ± 0.02 (7.18)

*Selectivity index (SI) = IC_{50} MCF-7/ IC_{50} Hek293-T

Kinetic studies were undertaken on compounds **3a**, **3h** and **4a** in order to elucidate the plausible mechanism of inhibition of α -glucosidase by these compounds.

2.2.4 Kinetic studies of **3a**, **3h** and **4a** against α -glucosidase

The mechanism of action of compounds **3a**, **3h** and **4a** against α -glucosidase was evaluated by building the Lineweaver–Burk double reciprocal plots and the Dixon plots at increasing inhibitor and substrate concentrations (0.1, 0.5, 2.5 and 5 μ M). Results of the Lineweaver-Burke plots represented in Figures 1a, 2a and 3a show relatively unchanged Michaelis constant (K_m) values of 0.020 ± 0.008 , 0.017 ± 0.007 , 0.019 ± 0.009 for **3a**, **3h** and **4a**, respectively. The maximum velocity of reaction (V_{max}) values for the three compounds decrease with increasing inhibitor concentration (0.02 μ M to 1 μ M) and these changes are as follows: 0.11 ± 0.013 to 0.022 ± 0.011 for **3a**, 0.10 ± 0.021 to 0.053 ± 0.021 for **3h**, and 0.10 ± 0.034 to 0.01 ± 0.004 for **4a**. Unchanged K_m and decreasing V_{max} values are indicative of non-competitive mode of inhibition. The Dixon plots for **3a** (Figure 1b), **3h** (Figure 2b) and **4a** (Figure 3b) all display intercepting lines above the x-axis, which is indicative of competitive mode of inhibition. This observation then supports mixed inhibition mode for **3a**, **3h** and **4a** suggesting that they bind to the active site and elsewhere on the enzyme. The calculated K_i values for **3a**, **3h** and **4a** are 0.13 ± 0.05 , 0.13 ± 0.01 and 0.17 ± 0.007 , respectively.

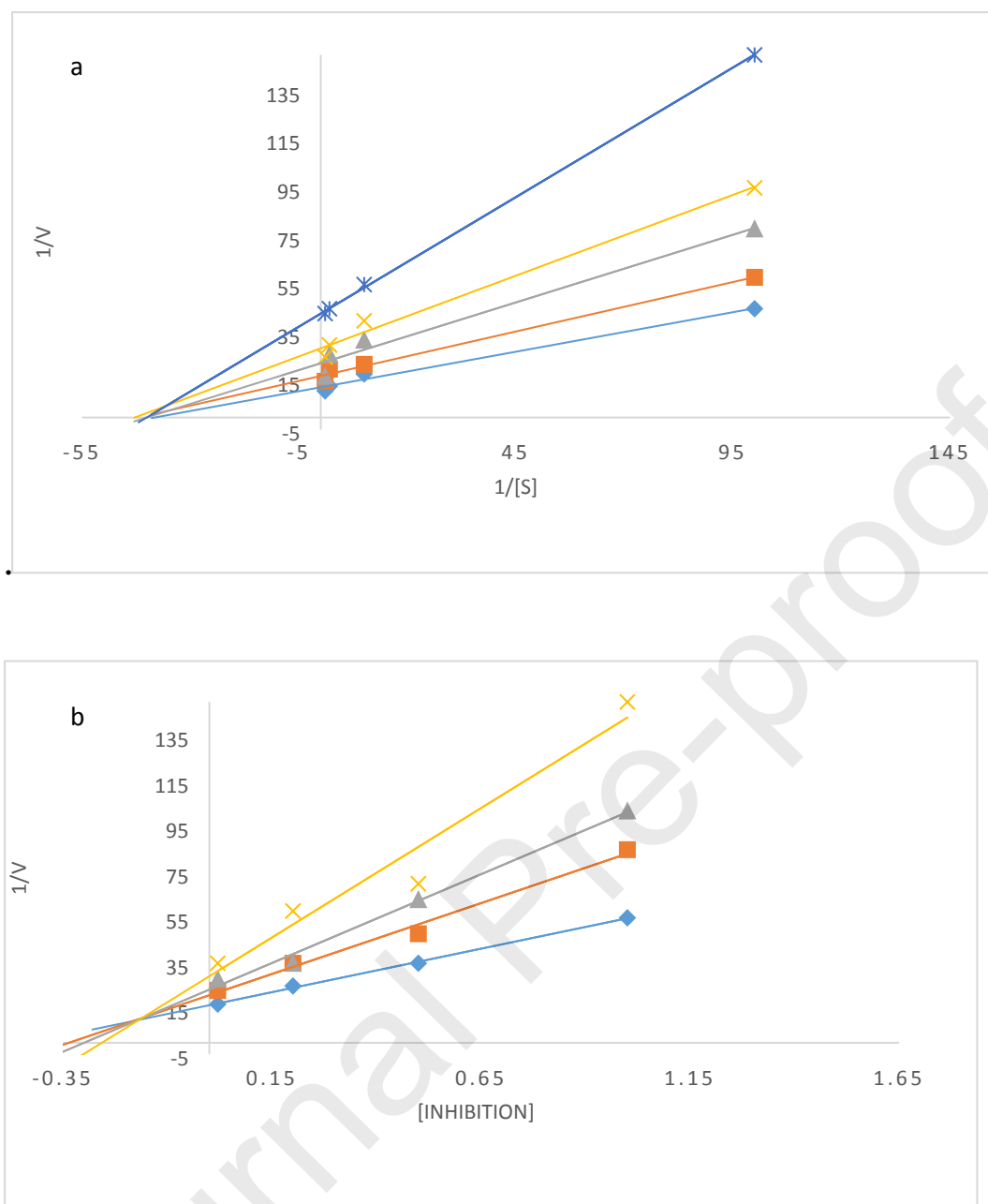


Figure 1: Lineweaver Burke (1a) and Dixon (1b) plots for compound **3a**. In the Lineweaver Burke plot inhibitor concentrations 0 μM , 0.02 μM , 0.2 μM and 0.5 μM are represented by blue, orange, grey and yellow symbols and lines, respectively. For the Dixon plot varying substrate concentrations of 0.01 μM , 0.1 μM , 0.5 μM and 1 μM are represented by yellow, grey, orange and blue symbols and lines respectively.

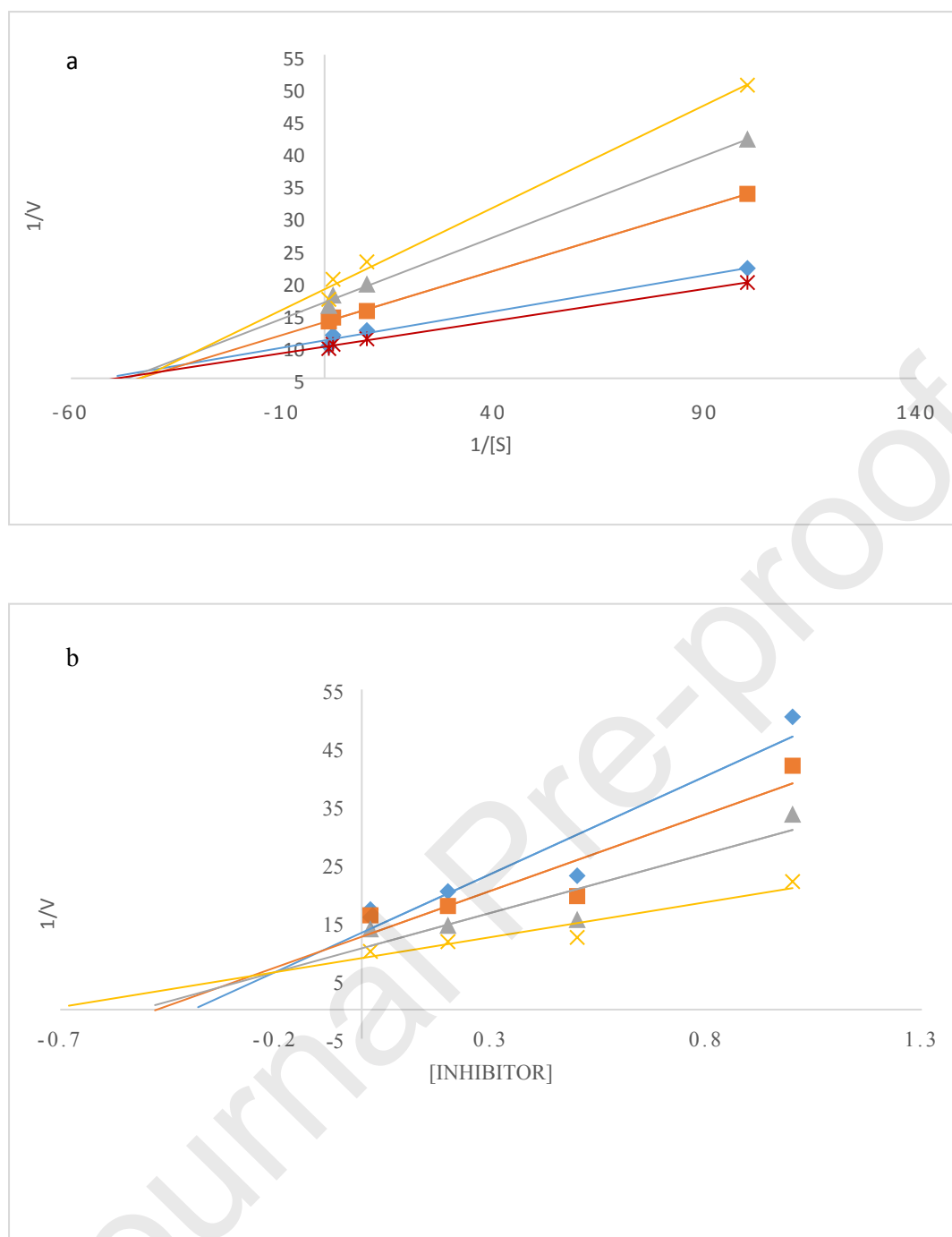


Figure 2: Lineweaver Burke (2a) and Dixon (2b) plots for compound **3h**. In the Lineweaver Burke plot inhibitor concentrations 0 μM , 0.01 μM , 0.1 μM , 0.5 μM and 1 μM are represented by red, blue orange, grey and yellow symbols and lines, respectively. For the Dixon plot varying substrate concentrations of 0.01 μM , 0.1 μM , 0.5 μM and 1 μM are represented by blue, orange, grey and yellow symbols and lines respectively.

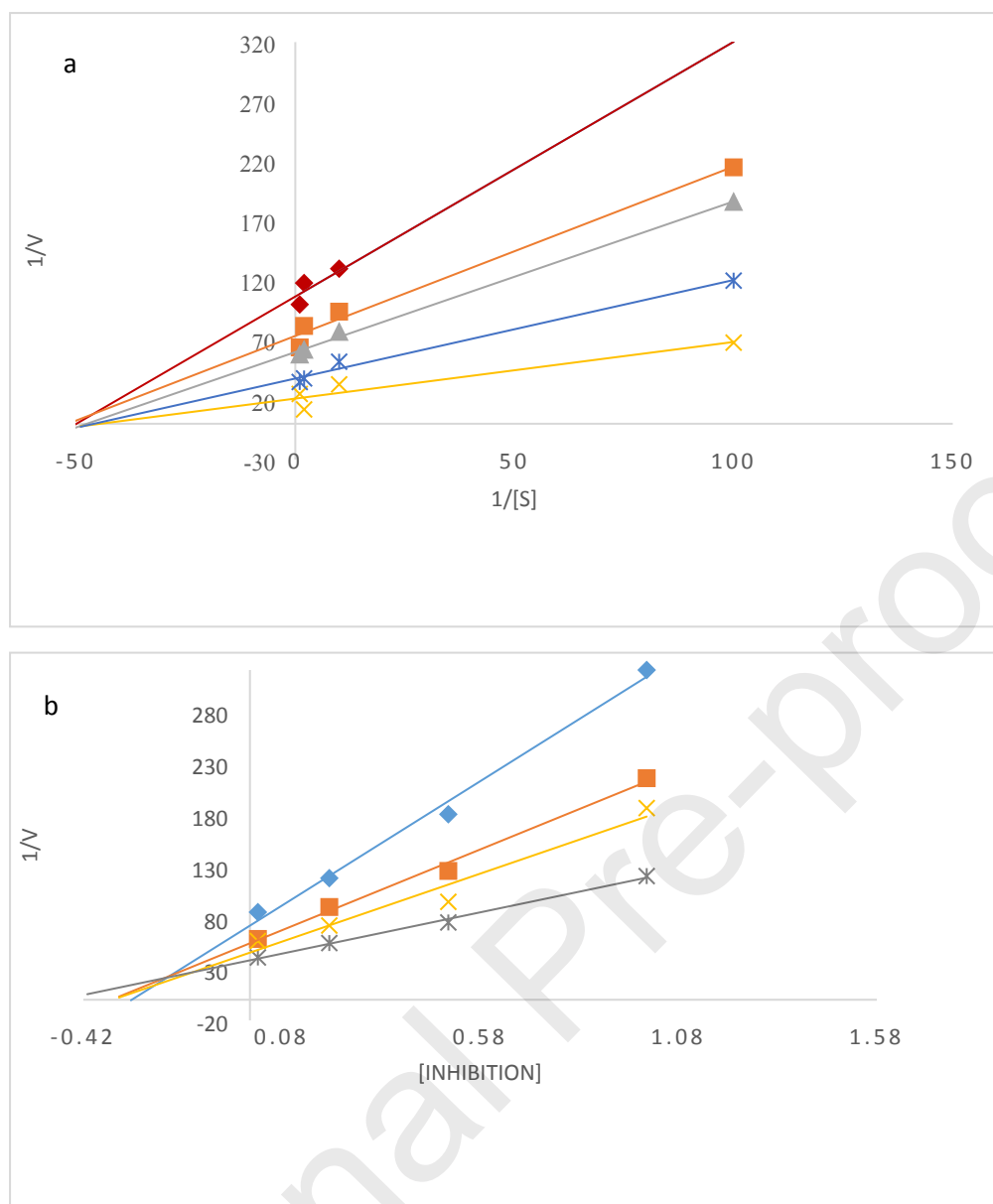


Figure 3: Lineweaver Burke (3a) and Dixon (3b) plots for compound **4a**. In the Lineweaver Burke plot inhibitor concentrations 0 μM , 0.02 μM , 0.2 μM , 0.5 μM and 1 μM are represented by yellow, red, blue, grey, orange and red symbols and lines, respectively. For the Dixon plot varying substrate concentrations of 0.01 μM , 0.1 μM , 0.5 μM and 1 μM are represented by blue, orange, yellow and grey symbols and lines, respectively.

To elucidate the protein-ligand interactions at molecular level, we performed a docking study on the most active compounds **3a**, **3e**, **3h**, **3k** and **4a** against the human lysosomal acid α -glucosidase.

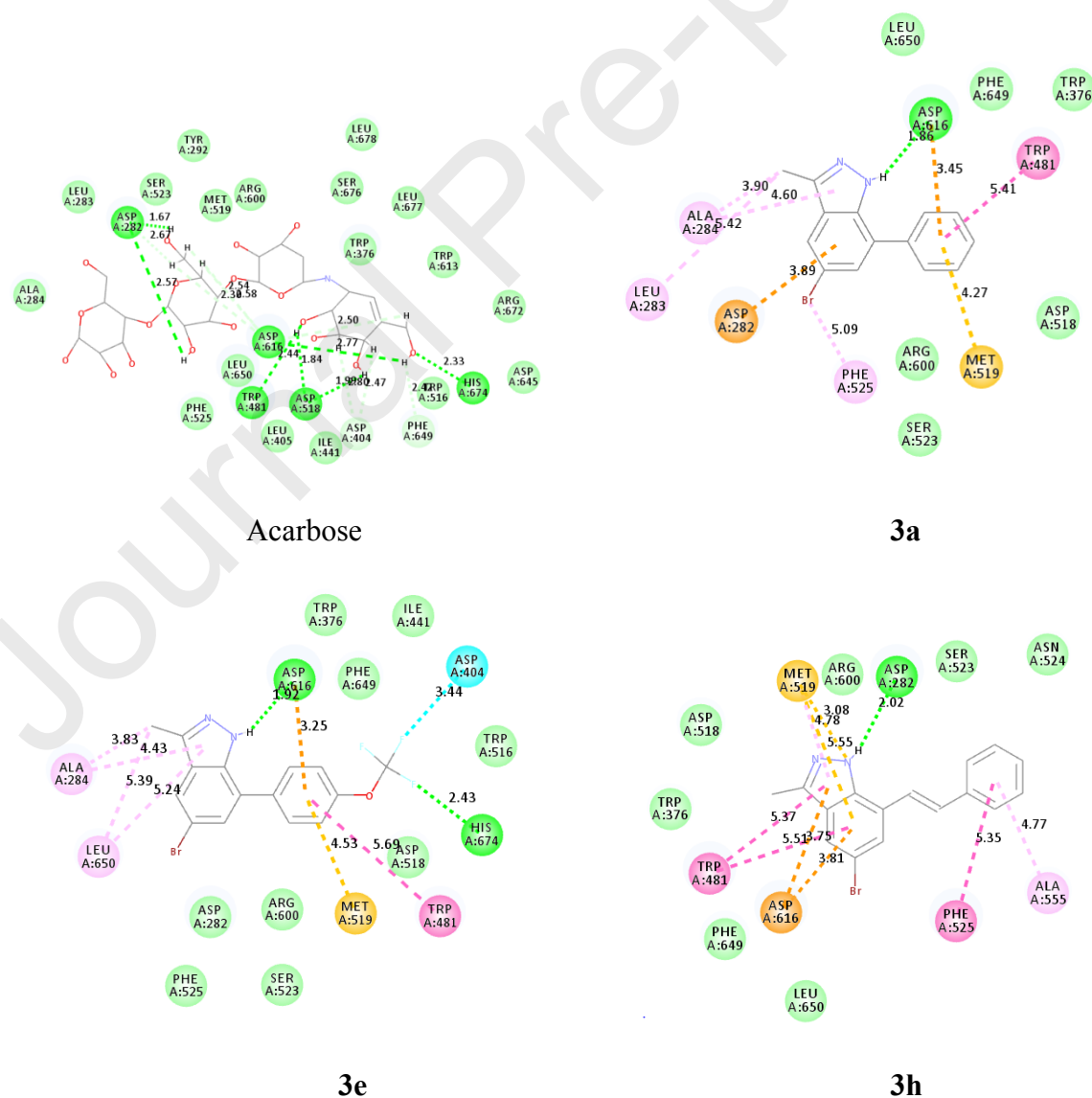
2.2.5 Molecular docking studies of **3a**, **3e**, **3h**, **3k** and **4a**

The X-ray crystal structure of human lysosomal acid α -glucosidase complexed with acarbose was downloaded from Protein Data Bank (PDB code: 5NN8). Acarbose was docked into the active site of this crystal and the top scoring docked pose with the calculated binding free energy (BE) of -88.6514 kcal/mol was applied as starting point for molecular dockings into α -glucosidase binding pocket. Interaction mode of acarbose with a human lysosomal acid- α -glucosidase revealed several hydrogen bonding interactions of this drug with the protein residues (Asp282, Asp518, Asp616, His674 and Trp481) in the active site of α -glucosidase (Figure 4a). Compounds **3a**, **3e**, **3h**, **3k** and **4a** were docked individually into the same active pocket site of α -glucosidase as acarbose, and their 2-dimensional docking poses showing interactions with the α -glucosidase protein residues and their distances are represented in Figure 4. The calculated BEs for **3a**, **3e**, **3h**, **3k** and **4a** are estimated to be -36.2257, -48.1500, -36.0903, -32.8335 and -41.0423 kcal/mol, respectively. These values are higher than that of acarbose, presumably because this reference drug has higher number of hydrogen bonding interactions with protein residues in the active site of α -glucosidase. The docking poses of **3a** (Figure 4b) and **3e** (Figure 4c) show the involvement of their heterocyclic ring in π -alkyl interaction with Ala284. The latter protein residue and Leu283 (**3a**) or Leu650 (**3e**) are involved in π -alkyl and alkyl interaction with the 3-methyl group, respectively. The 5-bromo atom of **3a** is involved in alkyl interaction with the protein residue Phe525. Hydrogen bonding interactions are predicted between the active site residue Asp616 and NH of both compounds. The phenyl ring in both cases is involved in π - π T-shaped interaction with Trp481, and also π -sulfur interaction with the protein residues Met519 and Asp616. Additional hydrogen bonding and halogen bonding interactions predicted between the trifluoromethoxy group with Asp404 and His674 help to increase the number of interactions with their protein targets, thereby enhancing biological activity of **3e** more so than the analogous 4-methoxyphenyl substituted derivative **3d**. These additional hydrophilic interactions probably account for the lower calculated BE value of **3e** among the test compounds. This compound has lower calculated BE value than **3a**,

which exhibited higher inhibitory effect against α -glucosidase activity among the 7-aryl substituted derivatives. The calculated binding energies obtained through molecular docking have been reported not to correlate well with the biological response observed in the *in vitro* tests [34].

The indazole scaffold of **3h** (Figure 4d) is involved in π - π T-shaped interaction with Trp481 and π -anion interactions with Asp616. There is π -sulphur and sulphur-x interactions between the fused benzene ring and N-1 with Met519, respectively. π -Alkyl interactions are predicted between the heterocyclic ring and Met519, and also between the styryl ring and Ala555. The styryl ring is also involved in π - π T-shaped interaction with Phe525. A hydrogen bond is predicted between the protein residue Asp282 and NH. The docking pose of **3k** (Figure 4e), on the other hand, shows the involvement of the heterocyclic ring in π -donor hydrogen bond interaction with the protein residue Ala284, which is also involved in π -alkyl interaction with the fused benzo ring. The 5-bromo atom of **3k** is involved in an alkyl interaction with Ala555, while its 3-methyl group is involved in a π -alkyl interaction with Leu283 and Ala284. The 4-methoxystyryl ring is involved in π - π T-shaped interaction with Trp481, π -sulphur interaction with Met519 and π -anion interactions with Asp616. Carbon hydrogen bonding interactions are predicted between the methoxy group of **3k** and protein residues Asp404 and Asp518. No hydrogen bonding is predicted between **3k** and the protein residues in the active site, which probably accounts for the high calculated BE value (-32.8335 kcal/mol) when compared to **3h** (-36.0903 kcal/mol). The enzyme-ligand complex for **3k** is stabilized by hydrophobic interactions (alkyl, π -alkyl and π - π T-shaped) and carbon hydrogen bonding interaction. The docking pose of **4a**, which is represented in Figure 5f shows both rings of the planar indazole scaffold involved in π -anion interaction with Asp616, and also π - π T-shaped interaction with Trp481. Met519 is involved in π -sulfur and sulphur-x interactions with the fused benzo ring and N-1, respectively. The heterocyclic ring of this compound is involved in π -alkyl interaction with Met519, while the 3-methyl group is involved in π -alkyl interaction

with Phe649. π - π T-shaped interaction and π -alkyl interaction exists between the phenyl ring with Phe525 and Ala555, respectively. Hydrogen bonding is predicted between NH and Asp282 as well as between N-2 and Arg600. Increased number of hydrophobic and hydrophilic interactions correlate well with enhanced inhibitory activity of this compound as well as its lowest calculated BE among the test compounds. Hydrophobic (alkyl, π -alkyl and π - π T shaped) and electrostatic (π -sulfur and/or π -anion) interactions, which are retained by these indazoles probably help anchor these compounds in the binding site of α -glucosidase, thereby enhancing their biological activity. These hydrophobic and electrostatic interactions, which are not established in acarbose- α -glucosidase complex presumably account for the higher activity of these indazole derivatives.



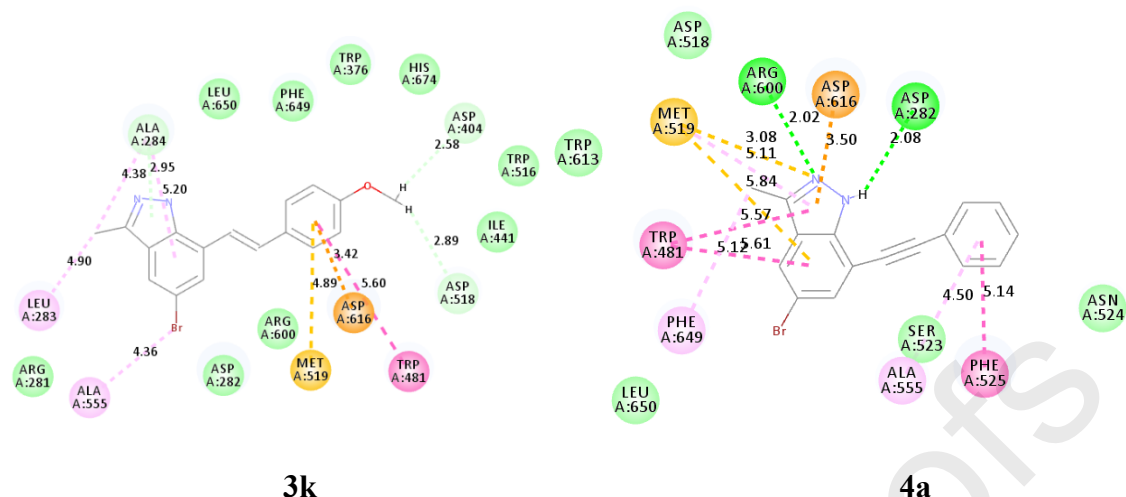


Figure 4. The predicted binding conformations of acarbose (4a) compounds **3a** (4b), **3e** (4c), **3h** (4d), **3k** (4e) and **4a** (4f and g) in the active site of α -glucosidase. Interactions with key amino acids are indicated with dashed lines (purple for hydrophobic contacts, green for H-bonds, and orange for charge attraction).

3. Conclusions

From a structure-activity-relationship perspective, among all the 7-carbo substituted 5-bromo-3-methylindazoles tested for the inhibition of α -glucosidase, derivatives in which the phenyl ring is linked directly (**3a**) or through a π -conjugated spacer such as C=C (**3h**) or C \equiv C (**4a**) bond exhibited increased inhibitory effect against α -glucosidase than all the other analogues and the trend is as follows: **4a** > **3h** > **3a**. The enzyme-ligand complexes appear to be stabilized by hydrophobic (alkyl, π -alkyl and π - π T-stacked), electrostatic and hydrophilic (hydrogen and/or halogen) bonding interactions. The presence of 5-bromo, 3-methyl and conjugated carbon-based substituent at the 7-position help to increase the number of hydrophobic interactions with protein residues in the active site of the human lysosomal acid α -glucosidase, thereby enhancing biological activity of these compounds. These compounds were also found to exhibit increased antioxidant activity in the DPPH free radical scavenging assay and the trend is as follows **4a** (IC₅₀ = 1.00 μ M) > **3a** (IC₅₀ = 4.99 μ M) > **3h** (IC₅₀ = 7.10

μM). Compounds **3a**, **3h** and **4a** were also found to exhibit moderate to increased cytotoxicity against the breast MCF-7 cancer cell line. Compound **4a** exhibited strong inhibition of the α -glucosidase enzyme than acarbose, the most robust antioxidant activity in comparison with ascorbic acid, and significant cytotoxicity against the MCF-7 cell line than doxorubicin. This compound exhibits multiple biological activities, which carries great potential for the therapy and prevention of diabetes and oxidative stress as well as cancer.

4. Experimental

4.1. General

The melting points of the prepared compounds were recorded on a Thermocouple digital melting point apparatus (Mettler Toledo LLC, Columbus, Ohio, USA) and are uncorrected. Their IR spectra were recorded as powders on a Bruker VERTEX 70 FT-IR Spectrometer (Bruker Optics, Billerica, MA, USA) with a diamond ATR (attenuated total reflectance) accessory by using the thin-film method. The Merck kieselgel 60 (0.063–0.200 mm) (Merck KGaA, Frankfurt, Germany) was used as stationary phase for column chromatography. The ^1H - and ^{13}C -NMR spectra of the prepared compounds were obtained as $\text{DMSO-}d_6$ solutions using the Varian Mercury 300 MHz NMR spectrometer (Agilent Technologies, Oxford, UK) and the chemical shifts are quoted relative to the tetramethylsilane (TMS) peak. The high-resolution mass spectra were recorded using a Waters Synapt G2 Quadrupole Time-of-flight mass spectrometer (Waters Corp., Milford, MA, USA) at an ionization potential of 70 eV. The synthesis and analytical data for 2-amino-5-bromo-3-iodoacetophenone, which has been used as a precursor in this investigation were reported in our previous investigation [35].

4.2.1. Synthesis of 1-(2-amino-5-bromo-3-iodophenyl)ethanone oxime (**1**)

A stirred mixture of 2-amino-5-bromo-3-iodoacetophenone (2.00 g, 5.90 mmol) in pyridine (30 mL) was treated slowly with ammonium hydroxyl chloride (0.49 g, 7.05 mmol), and then

heated under reflux for 2 h. Upon completion of the reaction (thin layer chromatography, TLC, monitoring), the mixture was allowed to cool and then quenched with an ice cold water. The resultant precipitate was filtered to afford **1** as a white solid (1.80 g, 80%), mp. 174–176 °C; ν_{\max} (ATR) 680, 755, 860, 1002, 1232, 1364, 1425, 1526, 1738, 2833, 3207, 3364 cm^{-1} ; $^1\text{H-NMR}$ (DMSO- d_6) 3.94 (3H, s, CH_3), 6.24 (2H, s, NH_2), 7.09 (1H, s, H-4), 7.36 (1H, s, H-6), 11.06 (1H, s, NH); $^{13}\text{C-NMR}$ (DMSO- d_6) 12.9, 86.9, 106.9, 120.5, 131.7, 140.3, 145.8, 155.1; HRMS (ES^+): m/z $[\text{M} + \text{H}]^+$ calcd for $\text{C}_8\text{H}_9\text{NO}^{79}\text{BrI}$: 353.8865; found 353.8863. Anal. Calcd for $\text{C}_8\text{H}_8\text{N}_2\text{OBrI}$: C, 27.07; H, 2.27; N, 7.89. Found: C, 27.04; H, 2.30; N, 7.93.

4.2.2. Synthesis of 5-bromo-7-iodo-3-methyl-1*H*-indazole (**2**)

A stirred mixture of 1-(2-amino-5-bromo-3-iodophenyl)ethanone oxime (2.00 g, 7.88 mmol) and triethylamine (1.60 g, 15.8 mmol) in dichloromethane (100 mL) at 0 °C was treated dropwise with a solution of methanesulfonyl chloride (1.01 g, 8.82 mmol) in dichloromethane (5 mL). The reaction was allowed to stir at room temperature (RT) for 4 h with thin layer chromatography (TLC) monitoring. Upon completion, the reaction mixture was quenched with an ice cold water. The aqueous phase was extracted with ethyl acetate (3 x 50 mL) and the combined organic layers were dried over anhydrous Na_2SO_4 . The salt was filtered off and the organic phase was concentrated under reduced pressure on a rotatory evaporator. The residue was purified by silica gel column chromatography eluting with 4:1 toluene-ethyl acetate (v/v) to afford **2** as a white solid (1.50 g, 58%), mp. 171–174 °C; ν_{\max} (ATR) 517, 601, 666, 703, 853, 907, 990, 1270, 1393, 2342, 2360, 2916, 3250 cm^{-1} ; $^1\text{H-NMR}$ (DMSO- d_6) 3.278 (3H, s, CH_3), 8.66 (1H, d, $J = 1.2$ Hz, H-4), 8.82 (1H, d, $J = 1.2$ Hz, H-6), 13.84 (1H, s, NH); $^{13}\text{C-NMR}$ (DMSO- d_6) 12.30, 76.38, 112.2, 122.9, 123.9, 136.5, 142.6, 142.7; HRMS (ES^+): m/z $[\text{M} + \text{H}]^+$ calcd for $\text{C}_8\text{H}_7\text{N}_2^{79}\text{BrI}$: 336.8759; found 336.8838. Anal. Calcd for $\text{C}_8\text{H}_6\text{N}_2\text{BrI}$: C, 28.52; H, 1.79; N, 8.31. Found: C, 28.49; H, 1.75; N, 8.33.

4.3. Typical procedure for the Suzuki-Miyaura cross-coupling of **2** to afford **3a–j**.

A mixture of **2** (1 equiv.), arylboronic acid (1.2 equiv.), PdCl₂(PPh₃)₂ (5 mol %), K₂CO₃ (1.5 equiv.) in 4:1 toluene-ethanol (v/v, 15 mL) was placed in a 2 necked flask equipped with a stirrer bar, rubber septum and a condenser. The mixture was flushed with argon gas for 5 min and a balloon filled with argon gas was connected to the top of a condenser. The mixture was then stirred at 80 °C for 5 h, cooled to room temperature and then quenched with an ice cold water. The product was extracted with chloroform and the combined organic layers were dried with MgSO₄, filtered and purified by silica gel column chromatography to afford **3** as a solid. The following compounds were prepared in this fashion:

4.3.1. 5-Bromo-3-methyl-7-phenyl-1*H*-indazole (**3a**)

Brown solid (0.22 g, 65%), mp. 162–165 °C; ν_{\max} (ATR) 603, 754, 851, 920, 987, 1257, 1316, 1478, 2853, 2922, 3234 cm⁻¹; ¹H-NMR (DMSO-*d*₆) 2.48 (3H, s, CH₃), 7.52–7.45 (2H, m, Ph), 7.55–7.52 (2H, m, H-4' and H-6), 7.66 (2H, d, *J* = 3.0 Hz, Ph), 7.69 (1H, d, *J* = 1.8 Hz, H-4), 12.95 (1H, s, NH); ¹³C-NMR (DMSO-*d*₆) 12.1, 112.7, 121.9, 125.3, 126.5, 127.9, 128.7, 129.3, 129.6, 136.6, 137.8, 141.9; HRMS (ES⁺): *m/z* [M + H]⁺ calcd for C₁₄H₁₂N₂⁷⁹Br: 287.0106; found 287.0184. Anal. Calcd for C₁₄H₁₁N₂Br: C, 58.56; H, 3.86; N, 9.76, Found: C, 58.55; H, 3.81; N, 9.73.

4.3.2. 5-Bromo-7-(4-fluorophenyl)-3-methyl-1*H*-indazole (**3b**)

Brown solid (0.29 g, 81%) mp. 205–207 °C; ν_{\max} (ATR) 602, 806, 835, 925, 1161, 1226, 1314, 1478, 1605, 2853, 2922, 3235 cm⁻¹; ¹H-NMR (DMSO-*d*₆) 2.57 (3H, s, CH₃), 7.54 (2H, dt, *J*_{HH} = 8.7 Hz and *J*_{HF} = 9.6 Hz, H-3', 5'), 7.63 (1H, d, *J* = 1.2 Hz, H-6), 7.87 (2H, dt, *J*_{HH} = 8.7 Hz and *J*_{HF} = 5.1 Hz, H-2', 6'), 7.93 (1H, d, *J* = 1.2 Hz, H-4), 13.0 (1H, s, NH); ¹³C-NMR (DMSO-*d*₆) 12.1, 112.7, 116.4 (d, ²*J*_{CF} = 20.6 Hz), 122.0, 125.2, 125.5, 128.0, 130.8 (d, ³*J*_{CF} = 8.0 Hz), 132.9 (d, ⁴*J*_{CF} = 2.7 Hz), 137.9, 141.9, 162.5 (d, ¹*J*_{CF} = 243.8 Hz); HRMS (ES⁺): *m/z* [M + H]⁺ calcd for C₁₄H₁₁N₂¹⁹F⁷⁹Br: 305.0011; found 305.0090. Anal. Calcd for C₁₄H₁₀N₂FBr: C, 55.10; H, 3.30; N, 9.18, Found: C, 55.00; H, 3.17; N, 9.20.

4.3.3. 5-Bromo-7-(4-chlorophenyl)-3-methyl-1*H*-indazole (**3c**)

White solid (0.25 g, 66%), mp. 199–201 °C; ν_{\max} (ATR) 693, 827, 923, 984, 1092, 1254, 1315, 1476, 1595, 2852, 2919, 3247 cm^{-1} ; $^1\text{H-NMR}$ (DMSO- d_6) 2.48 (3H, s, CH₃), 7.47 (1H, d, $J = 1.2$ Hz, H-6), 7.56 (2H, d, $J = 8.7$ Hz, H-3', 5'), 7.68 (2H, d, $J = 8.7$ Hz, H-2', 6'), 7.82 (1H, d, $J = 1.2$ Hz, H-4), 13.01 (1H, s, NH); $^{13}\text{C-NMR}$ (DMSO- d_6) 12.1, 112.7, 117.7, 122.6, 124.2, 125.3, 129.5, 129.6, 130.5, 130.9, 137.8, 142.0; HRMS (ES⁺): m/z [M + H]⁺ calcd for C₁₄H₁₁N₂³⁵Cl⁷⁹Br: 320.9716; found 320.9794. Anal. Calcd for C₁₄H₁₀N₂ClBr: C, 52.29; H, 3.13; N, 8.71, Found: C, 52.29; H, 3.10; N, 8.74.

4.3.4. 5-Bromo-7-(4-methoxyphenyl)-3-methyl-1*H*-indazole (**3d**)

White solid (0.20 g, 52%), mp. 179–182 °C; ν_{\max} (ATR) 700, 811, 836, 925, 990, 1033, 1177, 1247, 1439, 1503, 1605, 2852, 2921, 3246 cm^{-1} ; $^1\text{H-NMR}$ (DMSO- d_6) 2.48 (3H, s, CH₃), 3.81 (3H, s, OCH₃), 7.06 (2H, d, $J = 8.7$ Hz, H-3', 5'), 7.39 (1H, d, $J = 1.2$ Hz, H-6), 7.61 (2H, d, $J = 8.7$ Hz, H-2', 6'), 7.88 (1H, d, $J = 1.2$ Hz, H-4), 12.91 (1H, s, NH); $^{13}\text{C-NMR}$ (DMSO- d_6) 12.1, 55.7, 112.7, 114.7, 114.9, 121.3, 125.2, 127.4, 128.9, 129.9, 137.9, 141.8, 159.8; HRMS (ES⁺): m/z [M + H]⁺ calcd for C₁₅H₁₄N₂O⁷⁹Br: 317.0211; found 317.0290. Anal. Calcd for C₁₅H₁₃N₂OBr: C, 56.80; H, 4.13; N, 8.83; Found: C, 56.69; H, 4.12; N, 8.82.

4.3.5. 5-Bromo-7-(4-trifluoromethoxyphenyl)-3-methyl-1*H*-indazole (**3e**)

White solid (0.22 g, 50%), mp. 150–153 °C; ν_{\max} (ATR) 693, 836, 924, 1151, 1207, 1253, 1479, 1503, 2852, 2922, 3248 cm^{-1} ; $^1\text{H-NMR}$ (DMSO- d_6) 2.55 (3H, s, CH₃), 7.39 (2H, d, $J = 8.7$ Hz, H-3', 5'), 7.48 (1H, d, $J = 1.8$ Hz, H-6), 7.66 (2H, d, $J = 8.7$ Hz, H-2', 6'), 7.82 (1H, d, $J = 1.8$ Hz, H-4), 10.50 (1H, s, NH); $^{13}\text{C-NMR}$ (DMSO- d_6) 12.0, 113.7, 121.9, 122.2 (q, $J_{\text{CF}} = 256.5$ Hz), 122.2, 124.6, 124.9, 128.9, 129.3, 135.4, 137.9, 143.5, 149.2; HRMS (ES⁺): m/z [M + H]⁺ calcd for C₁₅H₁₁N₂OF₃⁷⁹Br: 371.0029; found 371.0007. Anal. Calcd for C₁₅H₁₀N₂OF₃Br: C, 48.54; H, 2.72; N, 7.55. Found: C, 48.52; H, 2.75; N, 7.52.

4.3.6. 5-Bromo-7-(3-aminocarbonylphenyl)-3-methyl-1*H*-indazole (**3f**)

White solid (0.25 g, 64%), mp. 199–202 °C; ν_{\max} (ATR) 644, 691, 939, 1123, 1261, 1569, 1674, 2852, 2921, 3149 cm^{-1} ; $^1\text{H-NMR}$ (DMSO- d_6) 2.50 (3H, s, CH₃), 7.21 (1H, t, $J = 7.8$ Hz,

H-5'), 7.48 (1H, d, $J = 1.2$ Hz, H-6), 7.55 (1H, dd, $J = 1.2$ and 7.8 Hz, H-6'), 7.61 (1H, d, $J = 1.2$ Hz, H-4), 7.82 (1H, d, 7.8 Hz, H-4'), 7.98 (1H, d, $J = 1.2$ Hz, H-2'), 8.10 (2H, s, NH₂), 13.02 (1H, s, NH); ¹³C-NMR (DMSO-*d*₆) 12.2, 112.7, 122.3, 125.8, 127.3, 128.0, 128.3, 128.7, 129.3, 129.6, 131.4, 135.8, 136.5, 137.8, 168.3; HRMS (ES⁺): m/z [M + H]⁺ calcd for C₁₅H₁₃N₂O⁷⁹Br: 330.0164; found 330.0242. *Anal* calcd for C₁₅H₁₂N₂OBr: C, 54.56; H, 3.66; N, 12.73. Found: C, 54.53; H, 3.63; N, 3.62.

4.3.7. 5-Bromo-7-(3-chloro-4-fluorophenyl)-3-methyl-1*H*-indazole (**3g**)

White solid (0.18 g, 51%), mp. 209–212 °C; ν_{\max} (ATR) 692, 834, 925, 987, 1235, 1313, 1478, 1798, 1602, 2853, 2922, 3238 cm⁻¹; ¹H-NMR (DMSO-*d*₆) 2.58 (3H, s, CH₃), 7.27 (1H, d, $J = 8.1$ Hz, H-5'), 7.33 (1H, t, $J = 2.1$ and 8.1 Hz, H-6'), 7.45 (1H, d, $J = 1.2$ Hz, H-6), 7.65 (1H, d, $J = 2.1$ Hz, H-2'), 7.83 (1H, d, $J = 1.2$ Hz, H-4); ¹³C-NMR (DMSO-*d*₆) 12.5, 112.9, 118.6 (d, ² $J_{\text{CF}} = 20.6$ Hz), 112.9, 123.3, 124.5, 125.6, 128.7 (d, ³ $J_{\text{CF}} = 6.7$ Hz), 129.8, 131.2, 134.5 (d, ⁴ $J_{\text{CF}} = 2.9$ Hz), 138.2, 142.1, 158.1 (d, ¹ $J_{\text{CF}} = 250.8$ Hz); HRMS (ES⁺): m/z [M + H]⁺ calcd for C₁₄H₁₀N₂F³⁵Cl⁷⁹Br: 338.9622; found 338.9700. *Anal* calcd for C, 49.52; H, 2.67; Br, 23.53; Cl, 10.44; F, 5.59; N, 8.25. Found: C, 10.39; H, 5.54; N, 8.25.

4.3.8. 5-Bromo-3-methyl-7-styryl-1*H*-indazole (**3h**)

White solid (0.30 g, 67%), mp. 205–208 °C; ν_{\max} (ATR) 686, 734, 954, 1294, 1339, 1489, 1576, 1738, 2852, 2916, 3034, 3133 cm⁻¹; ¹H-NMR (DMSO-*d*₆) 2.48 (3H, s, CH₃), 7.32 (1H, d, $J = 7.2$ Hz, H-4'), 7.42 (2H, t, $J = 7.5$ Hz, H-3', 5'), 7.50 (1H, d, $J_{\text{trans}} = 16.0$ Hz, H_a), 7.60 (1H, d, $J_{\text{trans}} = 16.0$ Hz, H_b), 7.68 (2H, d, $J = 7.2$ Hz, H-2', 6'), 7.79 (1H, d, $J = 1.2$ Hz, H-6), 7.86 (1H, d, $J = 1.2$ Hz, H-4), 13.2 (1H, s, NH); ¹³C-NMR (DMSO-*d*₆) 12.12, 112.9, 121.9, 122.7, 122.8, 124.9, 125.0, 127.2, 128.6, 129.2, 131.6, 137.4, 138.2, 141.9; HRMS (ES⁺): m/z [M + H]⁺ calcd for C₁₆H₁₄N₂⁷⁹Br: 313.0262; found 313.0340. *Anal*. Calcd for C₁₆H₁₃N₂Br: C, 61.36; H, 4.18; N, 8.94. Found: C, 61.35; H, 4.14; N, 8.92.

4.4.9. 5-Bromo-7-(4-fluorostyryl)-3-methyl-1*H*-indazole (**3i**)

White solid (0.28 g, 56%), mp. 208–211 °C; ν_{\max} (ATR) 803, 891, 955, 1158, 1227, 1484, 1509, 1580, 1738, 2919, 3037, 3148 cm^{-1} ; $^1\text{H-NMR}$ (DMSO- d_6) 2.43 (3H, s, CH_3), 7.63 (2H, dd, $J_{\text{HH}} = 8.7$ Hz and $J_{\text{HF}} = 9.6$ Hz, H-3', 5'), 7.86 (1H, $J_{\text{trans}} = 16.0$ Hz, H_a), 7.92 (1H, $J_{\text{trans}} = 16.0$ Hz, H_b), 8.08 (2H, $J_{\text{HH}} = 8.7$ Hz and $J_{\text{HF}} = 5.4$ Hz, H-2', 6'), 8.12 (1H, d, $J = 1.2$ Hz, H-6), 8.22 (1H, d, $J = 1.2$ Hz, H-4), 13.4 (1H, s, NH); $^{13}\text{C-NMR}$ (DMSO- d_6) 12.1, 112.9, 116.2 (d, $^2J_{\text{CF}} = 21.7$ Hz), 121.9, 122.7, 122.8, 124.9, 125.1, 129.0 (d, $^3J_{\text{CF}} = 7.5$ Hz), 130.4, 134.0 (d, $^4J_{\text{CF}} = 2.9$ Hz), 138.2, 141.9, 162.9 (d, $^1J_{\text{CF}} = 245.0$ Hz); HRMS (ES $^+$): m/z [M + H] $^+$ calcd for $\text{C}_{16}\text{H}_{13}\text{N}_2\text{F}^{79}\text{Br}$: 331.0168; found 331.0247. Anal. Calcd for $\text{C}_{16}\text{H}_{12}\text{N}_2\text{BrF}$: C, 58.03; H, 3.65; N, 8.46. Found: C, 57.99; H, 3.67; N, 8.53.

4.4.10. 5-Bromo-7-(4-chlorostyryl)-3-methyl-1*H*-indazole (**3j**)

White solid (0.28 g, 54%), mp. 243–246 °C; ν_{\max} (ATR) 806, 843, 947, 1097, 1301, 1489, 1604, 2852, 2919, 3057, 3181 cm^{-1} ; $^1\text{H-NMR}$ (DMSO- d_6) 2.48 (3H, s, CH_3), 7.50 (2H, d, $J = 8.4$ Hz, H-3', 5'), 7.61 (1H, d, $J_{\text{trans}} = 16.0$ Hz, H_a), 7.68 (1H, d, $J_{\text{trans}} = 16.0$ Hz, H_b), 7.69 (2H, d, $J = 8.4$ Hz, H-2', 6'), 7.78 (1H, d, $J = 1.8$ Hz, H-6), 7.87 (1H, d, $J = 1.8$ Hz, H-4), 13.14 (1H, s, NH); $^{13}\text{C-NMR}$ (DMSO- d_6) 12.10, 112.8, 122.2, 122.5, 123.6, 125.0, 125.3, 128.8, 129.3, 130.2, 132.9, 136.4, 138.2, 141.9; HRMS (ES $^+$): m/z [M + H] $^+$ calcd for $\text{C}_{16}\text{H}_{13}\text{N}_2^{35}\text{Cl}^{79}\text{Br}$: 346.9872; found 346.9951. Anal. Calcd for $\text{C}_{16}\text{H}_{11}\text{N}_2\text{ClBr}$: C, 55.28; H, 3.48; Br, 22.98; N, 8.06. Found: C, 55.27; H, 22.94; N, 8.02.

4.4.11. 5-Bromo-7-(4-methoxystyryl)-3-methyl-1*H*-indazole (**3k**)

White solid (0.10 g, 50%), mp. 219–222 °C; ν_{\max} (ATR) 837, 1110, 1174, 1247, 1300, 1510, 1574, 1605, 1737, 2918, 3033, 3146 cm^{-1} ; $^1\text{H-NMR}$ (DMSO- d_6) 2.47 (3H, s, CH_3), 3.77 (3H, s, OCH_3), 6.98 (2H, d, $J = 8.7$ Hz, H-3', 5'), 7.44 (1H, d, $J_{\text{trans}} = 16.0$ Hz, H_a), 7.55 (1H, d, $J_{\text{trans}} = 16.0$ Hz, H_b), 7.61 (2H, d, $J = 9.0$ Hz, H-2', 6'), 7.72 (1H, d, $J = 2.1$ Hz, H-6), 7.80 (1H, d, $J = 2.1$ Hz, H-4), 13.1 (1H, s, NH); $^{13}\text{C-NMR}$ (DMSO- d_6) 12.1, 55.7, 112.9, 114.7, 120.3, 121.3, 123.2, 124.5, 124.9, 128.6, 130.3, 131.3, 138.2, 141.8, 159.8; HRMS (ES $^+$): m/z [M +

$\text{H}]^+$ calcd for $\text{C}_{17}\text{H}_{16}\text{N}_2\text{O}^{79}\text{Br}$: 343.0368; found 343.0446. Anal. Calcd for $\text{C}_{17}\text{H}_{15}\text{N}_2\text{OBr}$: C, 59.49; H, 4.41; N, 8.16; Found: C, 59.47; H, 4.44; N, 8.20.

4.4. Typical procedure for the Sonogashira cross-coupling of **2** to afford **4a–f**

A mixture of **2** (1.0 equiv), $\text{PdCl}_2(\text{PPh}_3)_2$ (5 mol %), CuI (10 mol %), terminal alkyne (1.5 equiv.) and K_2CO_3 (1.5 equiv.) in 4:1 THF-water mixture (v/v, 15 mL/mmol of **2**) in a two-necked round bottom flask equipped with a stirrer bar, rubber septum, and a condenser was flushed with argon gas for 5 minutes. A balloon filled with argon gas was connected to the top of the condenser and the mixture was stirred at room temperature for 3 h. The mixture was quenched with an ice cold water and the product was extracted with chloroform. The combined organic layers were dried over anhydrous Na_2SO_4 . The salt was filtered off and then the solvent was evaporated under reduced pressure on a rotatory evaporator. The residue was purified by column chromatography on silica gel to afford **4**. The following compounds were prepared in this fashion:

4.4.1. 5-Bromo-3-methyl-7-(phenylethynyl)-1*H*-indazole (**4a**)

Brown solid (0.28 g, 61%), mp 181–183.9 °C; ν_{max} (ATR) 685, 754, 847, 888, 988, 1287, 1321, 1489, 1576, 1597, 2214, 2923, 3158 cm^{-1} ; $^1\text{H-NMR}$ ($\text{DMSO-}d_6$) 2.50 (3H, s, CH_3), 7.47 (3H, t, $J = 3.9$ Hz, Ph), 7.63 (1H, d, $J = 1.2$ Hz, H-6), 7.71 (2H, t, $J = 3.9$ Hz, Ph), 8.04 (1H, d, $J = 1.8$ Hz, H-4); $^{13}\text{C-NMR}$ ($\text{DMSO-}d_6$) 12.2, 84.3, 95.5, 107.0, 111.6, 122.4, 124.2, 124.4, 129.3, 129.7, 129.2, 131.4, 140.1, 142.5; HRMS (ES^+): m/z $[\text{M} + \text{H}]^+$ calcd for $\text{C}_{16}\text{H}_{12}\text{N}_2^{79}\text{Br}$: 311.0106; found 311.0184. Anal. Calcd for $\text{C}_{16}\text{H}_{11}\text{N}_2\text{Br}$: C, 61.76; H, 3.56; N, 9.00, Found: C, 61.77; H, 3.56; N, 8.96.

4.4.2. 5-Bromo-7-(3-fluorophenylethynyl)-3-methyl-1*H*-indazole (**4b**)

White solid (0.39 g, 76%), mp 215–217 °C; ν_{max} (ATR) 688, 777, 856, 871, 922, 1292, 1467, 1578, 1604, 2918, 3160 cm^{-1} ; $^1\text{H-NMR}$ ($\text{DMSO-}d_6$) 2.48 (3H, s, CH_3), 7.31–7.35 (1H, m, H-4'), 7.49–7.51 (2H, m, H-2' and H-6'), 7.54–7.65 (2H, m, H-5' and H-6), 8.06 (1H, d, $J = 1.8$ Hz, H-4), 13.38 (1H, s, NH); $^{13}\text{C-NMR}$ ($\text{DMSO-}d_6$) 12.2, 85.2, 94.2, 106.5, 111.6, 116.9

(d, $^2J_{CF} = 21.9$ Hz), 118.8 (d, $^2J_{CF} = 22.9$ Hz), 124.5 (d, $^3J_{CF} = 8.03$ Hz), 124.6, 128.4 (d, $^4J_{CF} = 2.7$ Hz), 131.3 (d, $^3J_{CF} = 8.03$ Hz), 131.4, 131.6, 140.2, 142.6, 163.9 (d, $^1J_{CF} = 248.8$ Hz); HRMS (ES⁺): m/z [M + H]⁺ calcd for C₁₆H₁₁N₂F⁷⁹Br: 329.0011; found 329.0090. Anal. Calcd for C₁₆H₁₀N₂BrF: C, 58.38; H, 3.06; N, 8.51. Found: C, 58.41; H, 3.11; N, 8.46.

4.4.3. 5-Bromo-7-(4-fluorophenylethynyl)-3-methyl-1H-indazole (**4c**)

White solid (0.33 g, 64%), mp. 204–206 °C; ν_{\max} (ATR) 831, 991, 1231, 1468, 1511, 1583, 2921, 3220 cm⁻¹; ¹H-NMR (DMSO-*d*₆) 1.35 (3H, s, CH₃), 6.16 (2H, dt, $J_{HH} = 8.7$ Hz and $J_{HF} = 9.7$ Hz, H-3', 5'), 6.48 (1H, d, $J = 1.8$ Hz, H-6), 6.65 (2H, dt, $J_{HH} = 8.7$ Hz and $J_{HF} = 5.4$ Hz, H-2', 6'), 6.89 (1H, d, $J = 1.8$ Hz, H-4), 12.22 (1H, s, NH); ¹³C-NMR (DMSO-*d*₆) 12.5, 84.4, 94.9, 107.3, 111.9, 116.9, (d, $^2J_{CF} = 21.8$ Hz), 119.2 (d, $^4J_{CF} = 2.7$ Hz), 124.5, 124.7, 131.7, 134.9 (d, $^3J_{CF} = 8.5$ Hz), 140.4, 142.8, 162.4 (d, $^4J_{CF} = 245.2$ Hz); HRMS (ES⁺): m/z [M + H]⁺ calcd for C₁₆H₁₁N₂F⁷⁹Br: 329.0011; found 329.0090. Anal calcd for C₁₆H₁₀N₂FBr: C, 58.38; H, 3.06; N, 8.51. Found: C, 58.29; H, 3.02; N, 8.47.

4.4.4. 5-Bromo-7-(3-chlorophenylethynyl)-3-methyl-1H-indazole (**4d**)

White solid (0.37 g, 72%), mp. 226–229 °C; ν_{\max} (ATR) 715, 758, 859, 881, 899, 1090, 1270, 1290, 1318, 1474, 1592, 2921, 3034 cm⁻¹; ¹H-NMR (DMSO-*d*₆) 2.50 (3H, s, CH₃), 7.47–7.49 (2H, m, Ar), 7.65 (2H, overlapping signals, Ar'), 7.89 (1H, d, $J = 1.2$ Hz, H-6), 8.01 (1H, d, $J = 1.2$ Hz, H-4), 13.4 (1H, s, NH); ¹³C-NMR (DMSO-*d*₆) 12.2, 85.5, 93.9, 106.5, 111.6, 124.4, 124.4, 124.6, 129.7, 130.6, 131.1, 131.6, 131.7, 133.7, 140.2, 142.6; HRMS (ES⁺): m/z [M + H]⁺ calcd for C₁₆H₁₁N₂³⁵Cl⁷⁹Br: 344.9716; found 344.9794. Anal. Calcd for C₁₆H₁₀N₂ClBr: C, 55.60; H, 2.92; N, 8.11. Found: C, 55.57; H, 2.95; N, 8.21.

4.4.5. 5-Bromo-7-(4-chlorophenylethynyl)-3-methyl-1H-indazole (**4e**)

White solid (0.32 g, 69%), mp. 225–228 °C; ν_{\max} (ATR) 710, 716, 823, 885, 989, 1092, 1268, 1317, 1466, 1488, 1580, 2921, 3214 cm⁻¹; ¹H-NMR (DMSO-*d*₆) 2.48 (3H, s, CH₃), 7.54 (2H, d, $J = 8.1$ Hz, H-3', 5'), 7.63 (1H, d, $J = 1.2$ Hz, H-6), 7.74 (2H, d, $J = 8.1$ Hz, H-2', 6'), 8.04 (1H, d, $J = 1.2$ Hz, H-4), 13.39 (1H, s, NH); ¹³C-NMR (DMSO-*d*₆) 12.2, 85.3, 94.4, 106.7,

106.7, 111.6, 121.3, 124.4, 129.4, 131.5, 133.8, 134.4, 140.1, 142.5; HRMS (ES⁺): m/z [M + H]⁺ calcd for C₁₆H₁₁N₂³⁵Cl⁷⁹Br: 344.9776; found 344.9794. Anal. Calcd for C₁₆H₁₀N₂ClBr: C, 55.60; H, 2.92; N, 8.11. Found: C, 55.58; H, 2.93; N, 8.14.

4.4.6. 5-Bromo-7-(4-methoxyphenylethynyl)-3-methyl-1*H*-indazole (**4f**)

White solid (0.36 g, 78%), mp. 172–175 °C; ν_{\max} (ATR) 828, 888, 1030, 1172, 1247, 1292, 1570, 1578, 1604, 2208, 2919, 3132 cm⁻¹; ¹H-NMR (DMSO-*d*₆) 2.49 (3H, s, CH₃), 3.80 (3H, s, OCH₃), 7.01 (2H, d, J = 8.7 Hz, H-3', 5'), 7.58 (1H, d, J = 1.2 Hz, H-6), 7.67 (2H, d, J = 8.7 Hz, H-2', 6'), 7.99 (1H, d, J = 1.2 Hz, H-4), 13.34 (1H, s, NH); ¹³C-NMR (DMSO-*d*₆) 12.2, 55.8, 83.0, 95.9, 107.6, 111.7, 114.3, 114.8, 123.6, 124.8, 130.9, 133.8, 140.0, 142.4, 160.3; HRMS (ES⁺): m/z [M + H]⁺ calcd for C₁₇H₁₄N₂O⁷⁹Br: 341.0211; found 341.0290. Anal. Calcd for C₁₇H₁₃N₂OBr: C, 59.84; H, 3.84; N, 8.21. Found: C, 59.80; H, 3.85; N, 8.23.

4.5. Inhibition of α -glucosidase activity

The α -glucosidase inhibitory activity of all synthetic compounds was assayed according to the modified procedure by Shi *et al.* [36] with slight modification. α -Glucosidase type1 from baker's yeast (G5003), *p*-nitrophenyl- α -D-glucopyranoside (N1377), acarbose (A8980) were purchased from Sigma Aldrich (Pty) Ltd. (Modderfontein, Johannesburg, South Africa). The stock solutions of the test compounds (500 μ M) were prepared in DMSO followed by dilution with 100 mM phosphate buffer to obtain the concentrations of 200 μ M. The selected assay concentrations for the test compounds (**2**, **3a–k** & **4a–f**) and acarbose as positive control were 1, 5, 10, 25 and 50 μ M. The enzyme solution (0.48 u/mL α -glucosidase, 17 μ L); phosphate buffer (100 mM, pH 6.8; 50 μ L) and test sample in DMSO (17 μ L) were incubated at 37 °C for 10 minutes. After pre-incubation, 17 μ L of 2 mM PNP-G was added. All tests and analyses were performed in triplicates and the absorbances were recorded in a 96 well microplate at 400 nm using Varioskan flash microplate spectrophotometer (Thermo Scientific, Waltham, MA, USA). IC₅₀ value was defined as the concentration of compound exhibiting 50% inhibition of α -glucosidase activity under the assay conditions. The values were calculated by the nonlinear

regression analysis and expressed as the mean SD of three distinct experiments using graph pad prism.

4.6. Kinetic studies against α -glucosidase

Compounds **3a**, **3h** and **4a** were selected for the kinetics studies with various substrate concentrations. The experimental process of the enzyme inhibition kinetics was similar to the above-mentioned conditions with inhibitors concentrations of 0.02, 0.2, 0.5, 1 μ M, and the ranges of final substrate concentration were 0.01–1 mM. The type of inhibition was determined by using Lineweave-Burk plot (the inverse of velocity ($1/v$) against the inverse of the substrate concentration ($1/[S]$). The inhibitor constant was obtained by Dixon plot (the inverse of velocity ($1/v$) against concentration of inhibitor at each substrate concentration) [37].

$$\frac{1}{v_o} = \frac{1}{v_o} + \frac{1}{v_{\max}[S]}$$

4.7. DPPH Assays of Compounds **2**, **3a–k** and **4a–f**.

DPPH radical scavenging activity of compounds **2**, **3a–k** and **4a–f** was evaluated following the literature method [38]. Ascorbic acid (Sigma Aldrich, Saint Louis, Missouri, USA) was used as a positive control. The test compounds and control at various concentrations (0 μ M to 50 μ M) in DMSO were mixed with a solution of DPPH (0.20 mM) in methanol. The mixtures were incubated in the dark for 45 minutes and the absorbances were recorded at 512 nm using Varioskan flash microplate spectrophotometer reader. All tests and analyses were run in triplicate and averaged. The inhibition was calculated in terms of percentage using the following formula:

$$\text{DPPH radical scavenged (\%)} = \frac{\text{AbC} - \text{AbS}}{\text{AbC}} \times 100$$

where AbC is absorbance of control and AbS the absorbance of the test sample. A graph of percentage inhibition of free radical activity was plotted against concentration of the sample and the IC_{50} (compound concentration required to reduce the absorbance of the DPPH control solution by 50%) was obtained from the graph.

4.8. Cytotoxicity of **3a**, **3e**, **3h**, **3k** and **4a** against MCF-7 and Hek293-T cells.

The MCF-7 and Hek293-T cells were seeded in a 96-well plate at a density of 20×10^3 cells per well, and then incubated at 37 °C in 5% CO₂ to allow cell attachment. The medium was removed and replaced with fresh medium containing various concentrations (0.4, 0.8, 1.6, 6.25, 12.5, 25, 50 and 100 µM) of the test sample and Doxo. After incubation for 24 h, 10 µL MTT (5 mg/mL) was added to each well and the plate was further incubated for 4 h. The supernatant was removed, and 100 µL of DMSO was added to each well to dissolve the resulting formazan crystals. The absorbance was read at 570 nm using the Varioskan flash microplate spectrophotometer reader and the cell viability. The percentages of cell viability were used to determine the IC₅₀ values.

4.9. Molecular docking studies

The coordinates for the crystal structure of human α -glucosidase with inhibitor, acarbose bound to it was downloaded from the PDB (code 5NN8) and was prepared prior to docking using Discovery Studio software version 19.1.0.18287 (Accelrys, San Diego, USA) prepare protein protocol. Compounds and the reference inhibitor acarbose were drawn and prepared using the prepare ligand protocol. The binding site x, y and z coordinates used were -13.9306, -38.1671 and 95.2761 with binding sphere radius of 15. Docking was performed using the CDOCKER module and the top poses with the optimal CDOCKER and CDOCKER interaction energy, were used for binding energy calculations. The binding energy for the poses were then calculated using the binding energy tool with in situ ligand minimisations conducted allowing for flexing of binding site sphere atoms and a Generalised Born with Molecular Volume (GBMV) used for the implicit solvent model. The pose with the best binding energy was then selected.

Supplementary Information: S1 contains the ¹H- and ¹³C-NMR spectra of all the compounds.

Acknowledgements: The authors thank the University of South Africa and the National Research Foundation (NRF) in South Africa for financial assistance. We also thank the

University of Stellenbosch Central Analytical Facility (CAF) for mass spectrometric and elemental analyses.

Funding: This project was funded by the University of South Africa and the National Research Foundation (NRF) in South Africa (NRF GUN: 118554). The views and opinions expressed herein are those of the authors and not of the funding bodies.

Conflict of interest: The authors declare no conflict of interest.

References

1. World Health Organization. Diabetes Fact Sheet. Available online: <https://www.who.int/news-room/factsheets/detail/diabetes> (Accessed 04/11/2019).
2. M.F. Carroll, A. Gutierrez, M. Castro, D. Tsewang, D.S. Schade, Targeting postprandial hyperglycemia: a comparative study of insulin tropic agents in type 2 diabetes. *J. Clin. Endocrinol. Metab.* 88 (2003) 5248–5254.
3. L.M. Muller, K.J. Gorter, E. Hak, *et al.* Increased risk of common infections in patients with type 1 and type 2 diabetes mellitus. *Clin. Infect. Dis.* 41 (2005) 281–288.
4. S.K. Garg, H. Maurer, K. Reed, R. Selagamsetty, Diabetes and cancer: two diseases with obesity as a common risk factor. *Diabetes Obes. Metab.* 16 (2014) 97–110.
5. E. Giovannucci, D.M. Harlan, M.C. Archer, S.M. Gapstur, L.A. Habel, M. Pollak, J.G. Regensteiner, D. Yee, Diabetes and Cancer. *Diabetes Care* 33 (2010) 1674–1685.
6. S. Suh, K.-W. Kim, Diabetes and cancer: is diabetes causally related to cancer? *Diabetes Metab. J.* 35 (2011) 193–198.
7. S.M. Samuel, E. Varghese, S. Varghese, D. Büsselberg, Challenges and perspectives in the treatment of diabetes associated breast cancer. *Cancer Treatment Rev.* 70 (2018) 98–111.
8. C. Rosak, G. Mertes, Critical evaluation of the role of acarbose in the treatment of diabetes: patient considerations. *Diabetes Metab. Syndr. Obes.* 5 (2012) 357–367.

9. L. Zeng, G. Zhang, Y. Liao, D. Gong, Inhibitory mechanism of morin on α -glucosidase and its anti-glycation properties. *Food Funct.* 7 (2016) 3953–3963.
10. S.R. Joshi, E. Standl, N. Tong, *et al.* Therapeutic potential of α -glucosidase inhibitors in type 2 diabetes mellitus: an evidence-based review. *Expert Opin. Pharmacother.* 16 (2015) 1959–1981.
11. H. Bischoff, The mechanism of alpha-glucosidase inhibition in the management of diabetes. *Clin. Invest. Med.* 18 (1995) 303–311.
12. V. Rani, G. Deep, R.K. Singh, K. Palle, U.C.S. Yadav, Oxidative stress and metabolic disorders: Pathogenesis and therapeutic strategies. *Life Sci.* 148 (2016) 183–193.
13. R. Pili, J. Chang, R. Partis, *et al.* The α -glucosidase I inhibitor castanospermine alters endothelial cell glycosylation, prevents angiogenesis, and inhibits tumor growth. *Cancer Res.* 55 (1995) 2920–2926.
14. S. Tudzarova, M.A. Osman, The double trouble of metabolic diseases: the diabetes cancer link. *Mol. Biol. Cell* 26 (2015) 3129–39.
15. R.J. Patch, H. Huang, S. Patel, W. Cheung, G. Xu, B.-P. Zhao, D.A. Beauchamp, D. Rentzeperis, J.G. Geisler, H.B. Askari, J. Liu, J. Kasturi, M. Towers, M.D. Gaul, M.R. Player, Indazole-based ligands for estrogen-related receptor α as potential anti-diabetic agents. *Eur. J. Med. Chem.* 138 (2017) 830–853.
16. G. Taneja, G.P. Gupta, S. Mishra, R. Srivastava, N. Rahuja, *et al.* Synthesis of substituted 2*H*-benzo[*e*]indazole-9-carboxylate as a potential antihyperglycemic agent that may act through IRS-1 akt and GSK-3 β pathways. *Med. Chem. Commun.* 8 (2012) 329–337.
17. F. Song, G. Xu, M.D. Gaul, B. Zhao, T. Lu, *et al.* Design, synthesis and structure activity relationships of indazole and indole derivatives as potent glucagon receptor antagonists. *Bioorg. Med. Chem. Lett.* 29 (2019) 1974–1980.

18. D.D. Gaikwad, A.D. Chapolikar, C.G. Dekate, K.D. Warad, A.P. Tayade, R.P. Pawar, A. Domb, Synthesis of indazole motifs and their medicinal importance: An overview. *Eur. J. Med. Chem.* 90 (2015) 707–731.
19. J. Dong, Q. Zhang, Z. Wang, G. Huang, S. Li, Recent advances in the development of indazole-based anticancer agents. *ChemMedChem* 13 (2018) 1490–1507.
20. Y. Liu, L. Ma, W.-H. Chen, H. Park, Z. Ke, B. Wang, Binding mechanism and synergetic effects of xanthone derivatives as noncompetitive α -glucosidase inhibitors: a theoretical and experimental study. *J. Phys. Chem. B* 117 (2013) 13464–13471.
21. S. Qian, J. He, W. Huang, Y. He, M. Zhang, L. Yang, G. Li, Z. Wang, Discovery and preliminary structure–activity relationship of 1*H*-indazoles with promising indoleamine-2,3-dioxygenase 1 (IDO1) inhibition properties. *Bioorg. Med. Chem.* 24 (2016) 6194–6205.
22. R.D. Carpenter, A. Natarajan, E.Y. Lau, M. Andrei, D.M. Solano, F.C. Lightstone, S.J. DeNardo, K.S. Lam, M.J. Kurth, Halogenated benzimidazole carboxamides target integrin $\alpha(4)\beta(1)$ on T-cell and B-cell lymphomas. *Cancer Res.* 70 (2010) 5448–5456.
23. S. El Kazzouli, G. Guillaumet, Functionalization of indazoles by means of transition metal-catalyzed cross-coupling reactions. *Tetrahedron* 72 (2016) 6711–6727.
24. A. Ullah, A. Khan, I Khan, Diabetes mellitus and oxidative stress- A concise review. *Saudi Pharm. J.* 24 (2016) 547–553.
25. F.R. Leroux, B. Manteau¹, J.-P. Vors, S. Pazenok, Trifluoromethyl ethers – synthesis and properties of an unusual substituent. *Beilstein J. Org. Chem.* 4 (2008) doi:10.3762/bjoc.4.13.
26. R. Wilcken, M.O. Zimmermann, A. Lange, A.C. Joerger, F.M. Boeckler, Principles and applications of halogen bonding in medicinal chemistry and chemical biology. *J. Med. Chem.* 56 (2012) 1363–1388.

27. S.O. Famuyiwa, K. Sanusi, K.O. Faloye, Y. Yilmaz, U. Ceylan, Antidiabetic and antioxidant activities: Is there any link between them? *New. J. Chem.* 43 (2019) 13326–13329.
28. N. Matsuzawa-Nagata, T. Takamura, H. Ando, S. Nakamura, S. Kurita, H. Misu, T. Ota, M. Yokoyama, M. Honda, K. Miyamoto, S. Kaneko, Increased oxidative stress precedes the onset of high-fat diet-induced insulin resistance and obesity. *Metabolism* 57 (2008) 1071–1077.
29. M. Kunitomo, Y. Yamaguchi, S. Kagota, K. Otsubo, Beneficial effect of coenzyme Q10 on increased oxidative and nitrative stress and inflammation and individual metabolic components developing in a rat model of metabolic syndrome. *J. Pharmacol. Sci.* 107 (2008) 128–137.
30. C. Cheekavolu, M. Muniappan, *In vivo* and *in vitro* anti-inflammatory activity of indazole and its derivatives. *J. Clin. Diagn. Res.* 10 (2016) FF01-FF06.
31. V. Pavlovic, S. Cekic, G. Rankovic, N. Stoiljkovic, Antioxidant and pro-oxidant effect of ascorbic acid. *Acta Medica Medianae* 44 (2005) 65–68.
32. M.H.A. Aziz, N. Abu, S.K. Yeap, W.Y. Ho, A.R. Omar, N.H. Ismail, *et al.* Combinatorial cytotoxic effects of damnacanthol and doxorubicin against human breast cancer MCF-7 cells in Vitro. *Molecules* 21 (2016) 1228.
33. F. Benyettou, H. Fahs, R. Elkharrag, R.A. Bilbeisi, B. Asma, *et al.* Selective growth inhibition of cancer cells with doxorubicin-loaded CB[7]-modified iron-oxide nanoparticles. *RSC. Adv.* 7 (2017) 23827–23834.
34. A. Aispuro-Pérez, J. López-Ávalos, F. García-Páez, J. Montes-Avila, L.A. Picos-Corrales, *et al.* Synthesis and molecular docking studies of imines as α -glucosidase and α -amylase inhibitors. *Bioorg. Chem.* 94 (2020) 103491.
35. M.J. Mphahlele, T.J. Makhafola, M.M. Mmonwa, *In vitro* cytotoxicity of novel 2,5,7-tricarbo-substituted indoles derived from 2-amino-5-bromo-3-iodoacetophenone. *Bioorg. Med. Chem.* 24 (2016) 4576–4586.

36. Z.L. Shi, Y.D. Liu, Y.Y. Yuan, D. Song, M.F. Qi, X.J. Yang, P. Wang, X.Y. Li; J.H. Shang, Z.X. Yang, In vitro and in vivo effects of Norathyriol and Mangiferin on α -glucosidase. *Biochem. Res. Int.* (2017) 1–7.
37. R. Rafique, K.M. Khan, A. Kanwal, S. Chigurupati, A. Wadood, A.U. Rehman, A. Karunanidhi, S. Hameed, M. Taha, M. Rashida, Synthesis of new indazoles based dual inhibitors of α -glucosidase and α -amylase enzymes, their *in vitro*, *in silico* and kinetics studies. *Bioorg. Chem.* 94 (2019), 103195.
38. K. Zhu, H. Zhou, H. Qian, Antioxidant and free radical-scavenging activities of wheat germ protein hydrolysates (WGPH) prepared with alcalase. *Process Biochem.* 41 (2006) 1296–1302.

Declaration of interests

The authors declare that they have no known competing financial interests or personal relationships that could have appeared to influence the work reported in this paper.

The authors declare the following financial interests/personal relationships which may be considered as potential competing interests:

The authors declare no conflict of interest. The views and opinions expressed herein are those of the authors and not of the funding bodies.

Scheme 1: Suzuki-Miyaura and Sonogashira cross-coupling of **2** to afford **3a–k** and **4a–f**, respectively.

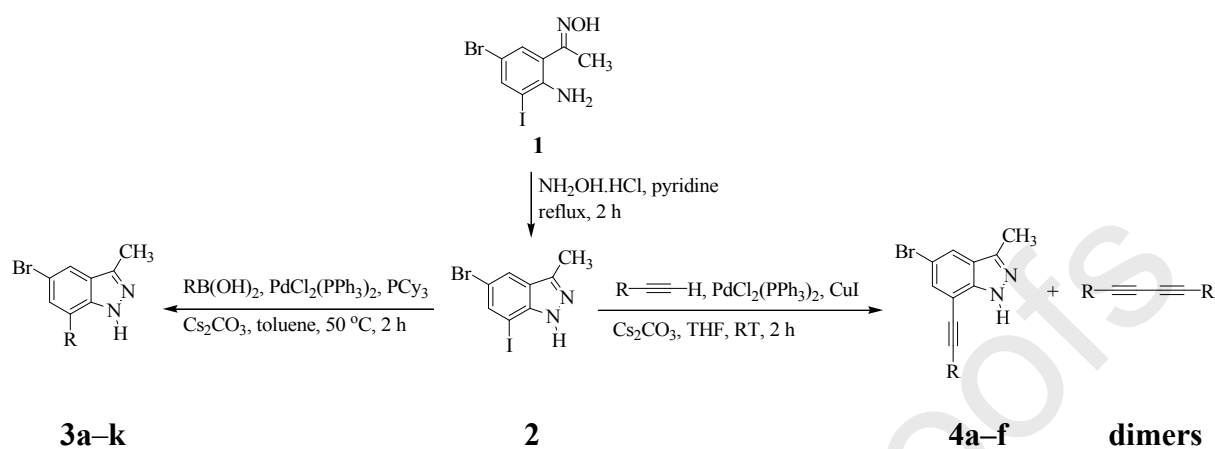


Table 1: Substitution patterns of compounds **3a–k** and **4a–f**.

3: R =	C ₆ H ₅ - (3a); 4-FC ₆ H ₄ - (3b); 4-ClC ₆ H ₄ - (3c); 4-MeOC ₆ H ₄ - (3d); 4-CF ₃ OC ₆ H ₄ - (3e); 4-NH ₂ C(O)C ₆ H ₄ - (3f); 3-Cl,4-FC ₆ H ₃ - (3g); PhCH=CH- (3h); 4-FC ₆ H ₄ CH=CH- (3i); 4-ClC ₆ H ₄ CH=CH- (3j); 4-CH ₃ OC ₆ H ₄ CH=CH- (3k)
4: R =	C ₆ H ₅ - (4a); 3-FC ₆ H ₄ - (4b); 4-FC ₆ H ₄ - (4c); 3-ClC ₆ H ₄ - (4d); 4-ClC ₆ H ₄ - (4e); 4-MeOC ₆ H ₄ - (4f)

Table 2: α -Glucosidase inhibitory and antioxidant activities of **2–4**, and cytotoxicity against **3a, 3e, 3h, 3k** and **4a**.

IC₅₀ values (μM)			
2–4	α-Glucosidase	DPPH	MCF-7
2	11.69 \pm 0.010	6.79 \pm 0.003	-
3a	0.53 \pm 0.013	4.99 \pm 0.006	49.90 \pm 0.02
3b	51.07 \pm 0.001	50.52 \pm 0.001	-
3c	22.68 \pm 0.001	0.91 \pm 0.004	-
3d	13.52 \pm 0.006	49.40 \pm 0.003	-
3e	0.75 \pm 0.006	4.84 \pm 0.009	71.94 \pm 0.05
3f	22.7 \pm 0.012	26.33 \pm 0.005	-
3g	5.49 \pm 0.003	4.62 \pm 0.005	-
3h	0.50 \pm 0.010	7.10 \pm 0.004	39.33 \pm 0.02
3i	51.51 \pm 0.013	15.30 \pm 0.003	-
3j	7.73 \pm 0.004	1.06 \pm 0.013	-
3k	0.80 \pm 0.009	14.46 \pm 0.009	53.25 \pm 0.05
4a	0.42 \pm 0.019	1.00 \pm 0.007	35.13 \pm 0.02
4b	7.14 \pm 0.009	88.66 \pm 0.001	-
4c	5.27 \pm 0.004	7.96 \pm 0.001	-
4d	3.42 \pm 0.002	66.20 \pm 0.01	-
4e	4.87 \pm 0.004	27.83 \pm 0.01	-
4f	23.71 \pm 0.004	4.92 \pm 0.01	-
Acarbose	0.82 \pm 0.006	-	-
Ascorbic acid	-	5.20 \pm 0.006	-
Gefitinib	-	-	36.03 \pm 0.02

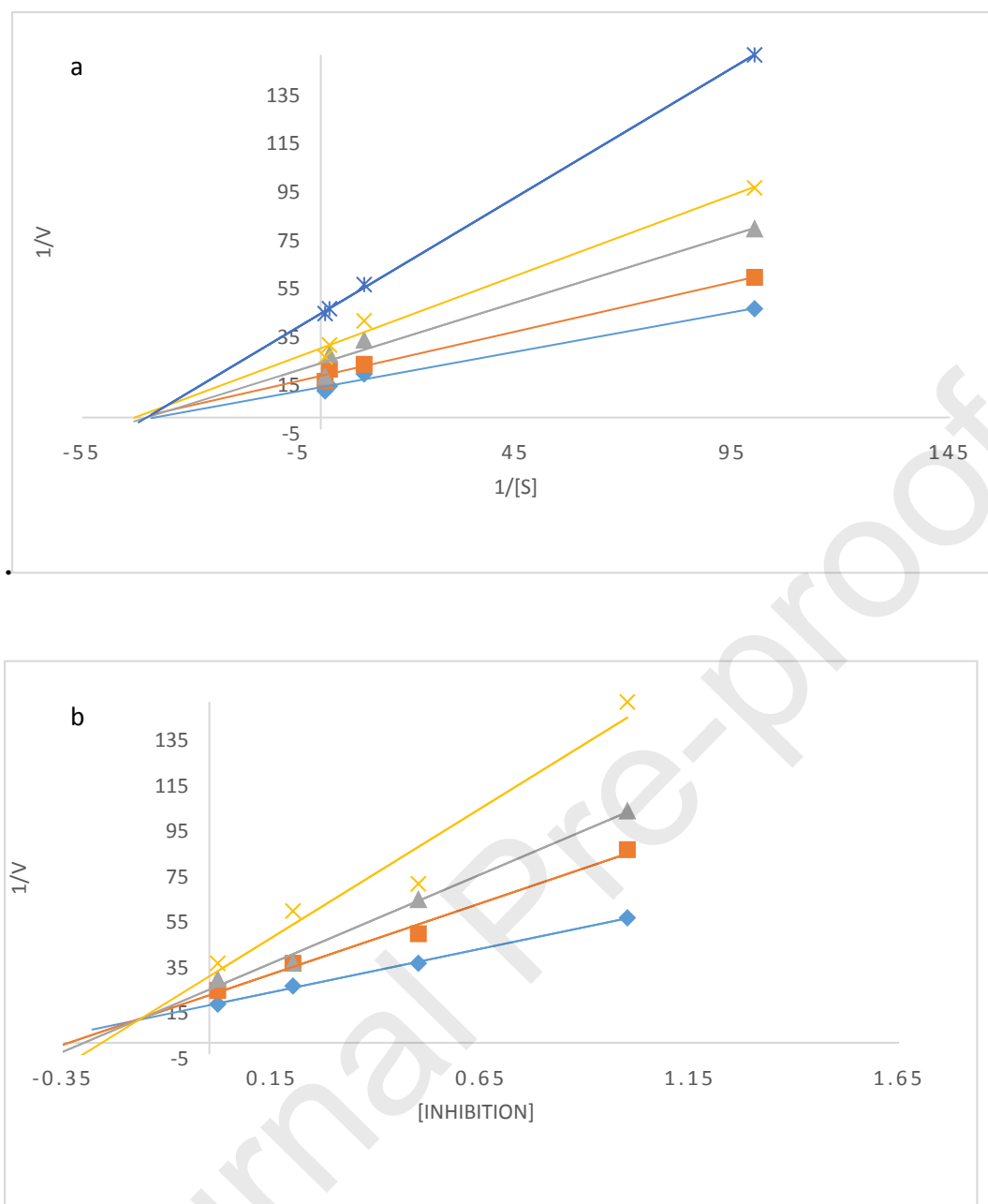


Figure 1: Lineweaver Burke (1a) and Dixon (1b) plots for compound **3a**. In the Lineweaver Burke plot inhibitor concentrations 0 μM , 0.02 μM , 0.2 μM and 0.5 μM are represented by blue, orange, grey and yellow symbols and lines, respectively. For the Dixon plot varying substrate concentrations of 0.01 μM , 0.1 μM , 0.5 μM and 1 μM are represented by yellow, grey, orange and blue symbols and lines respectively.

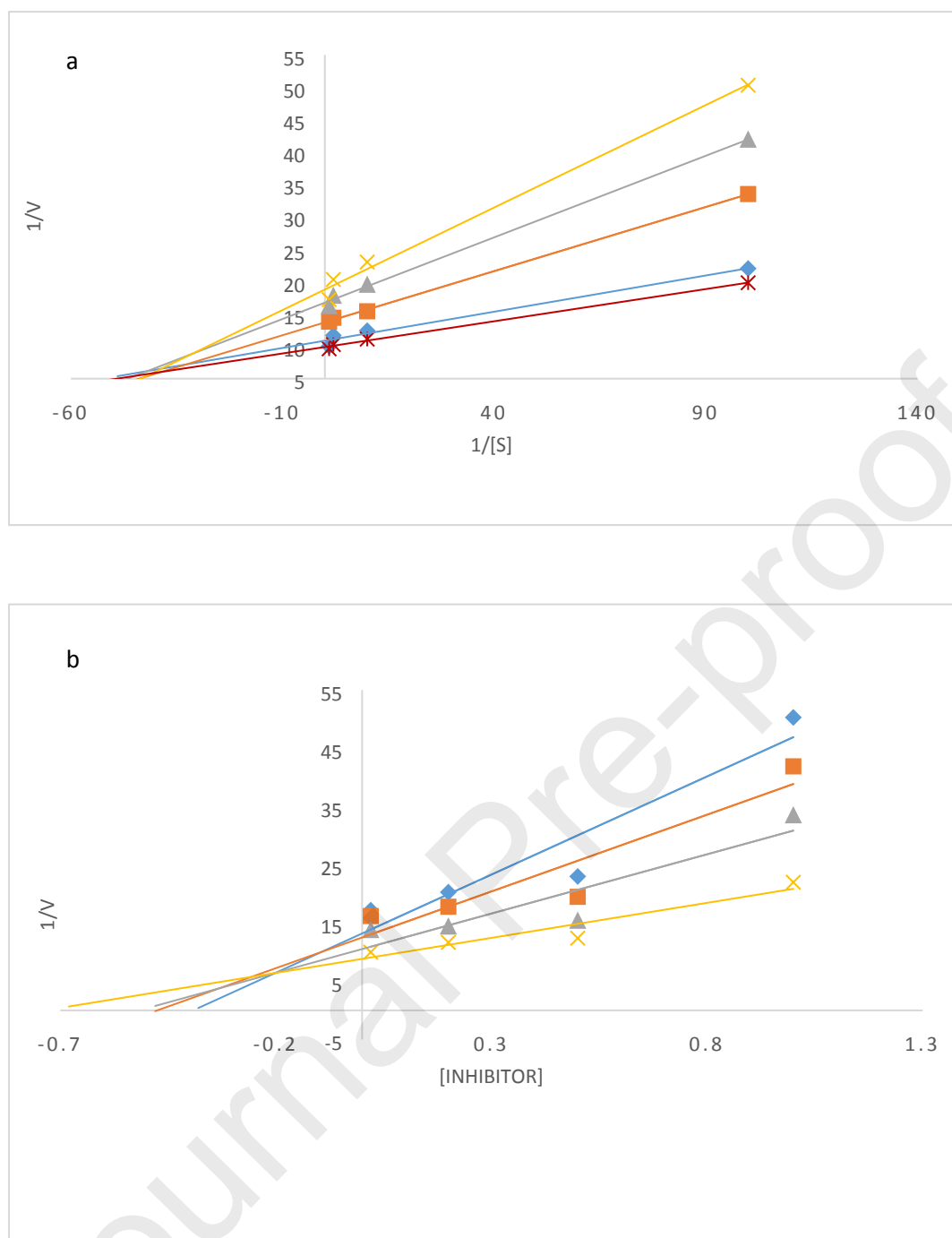


Figure 2: Lineweaver Burke (2a) and Dixon (2b) plots for compound **3h**. In the Lineweaver Burke plot inhibitor concentrations 0 μM , 0.01 μM , 0.1 μM , 0.5 μM and 1 μM are represented by red, blue orange, grey and yellow symbols and lines, respectively. For the Dixon plot varying substrate concentrations of 0.01 μM , 0.1 μM , 0.5 μM and 1 μM are represented by blue, orange, grey and yellow symbols and lines respectively.

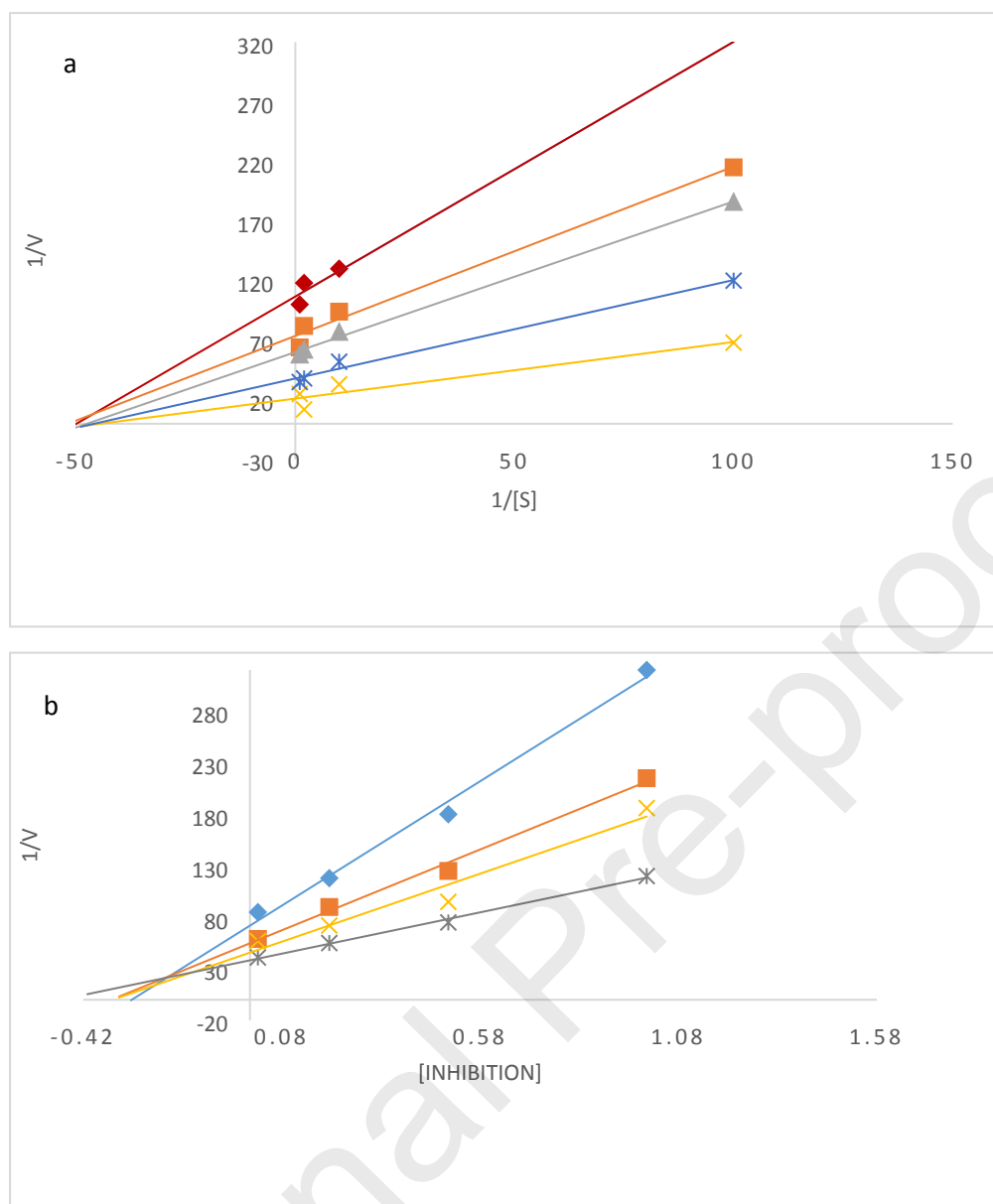
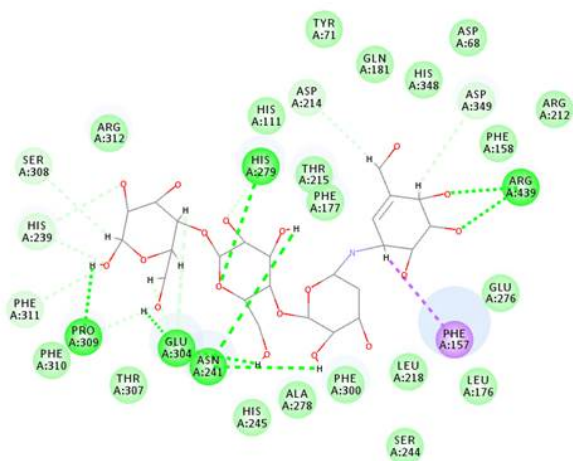
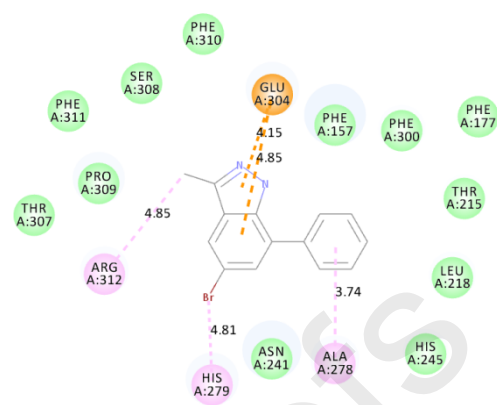


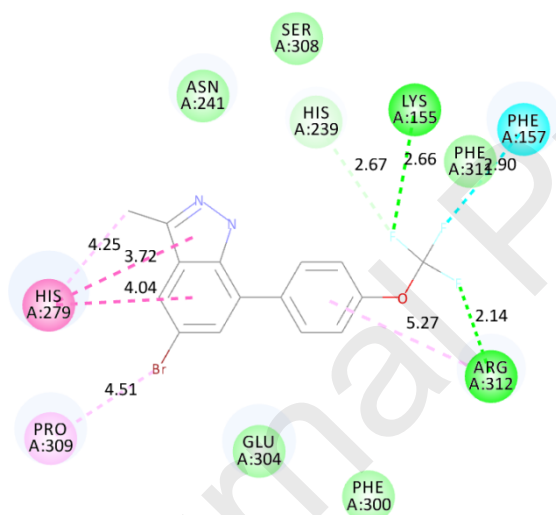
Figure 3: Lineweaver Burke (3a) and Dixon (3b) plots for compound **4a**. In the Lineweaver Burke plot inhibitor concentrations 0 μM , 0.02 μM , 0.2 μM , 0.5 μM and 1 μM are represented by yellow, red, blue, grey, orange and red symbols and lines, respectively. For the Dixon plot varying substrate concentrations of 0.01 μM , 0.1 μM , 0.5 μM and 1 μM are represented by blue, orange, yellow and grey symbols and lines, respectively.



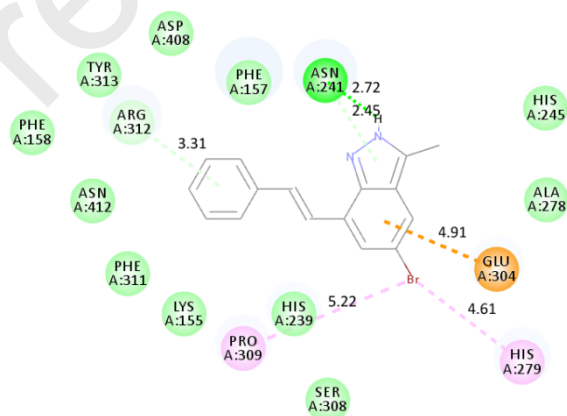
Acarbose



3a



3e



3h

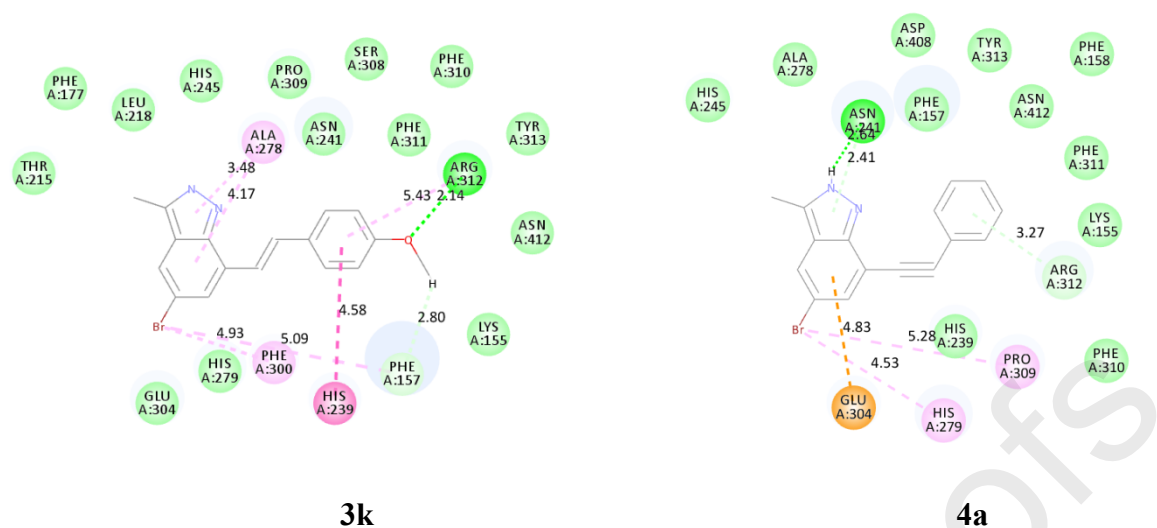
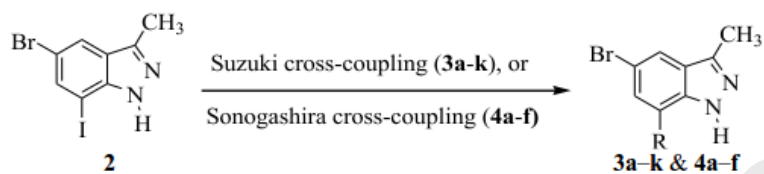
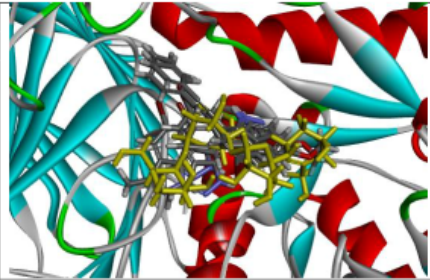


Figure 4. The predicted binding conformations of acarbose (4a) compounds **3a** (4b), **3e** (4c), **3h** (4d), **3k** (4e) and **4a** (4f) in the active site of α -glucosidase. Interactions with key amino acids are indicated with dashed lines (purple for hydrophobic contacts, green for H-bonds, light blue for halogen bonds, and orange for charge attraction).

Synthesis, α -glucosidase inhibition and antioxidant activity of the 7-carbo-substituted 5-bromo-3-methylindazoles



	3a: R = C ₆ H ₅ - 3h: R = C ₆ H ₅ CH=CH- 4a: R = C ₆ H ₅ C≡C-		
	IC ₅₀ values (μM)		
Compound	α -Glucosidase	DPPH	MCF-7
3a	0.53 ± 0.013	4.99 ± 0.006	49.90 ± 0.02
3h	0.50 ± 0.010	7.10 ± 0.004	39.33 ± 0.02
4a	0.42 ± 0.019	1.00 ± 0.007	35.13 ± 0.02
Acarbose	0.82 ± 0.006	-	-
Ascorbic acid	-	5.20 ± 0.006	-
Gefitinib	-	-	36.03 ± 0.02

Highlights:

- Series of 3,5,7-trisubstituted indazoles were prepared and evaluated against α -glucosidase
- Their antioxidant properties were evaluated through 2,2-diphenyl-1-picrylhydrazyl radical scavenging assay
- The most active compounds exhibit dual anti- α -glucosidase and antioxidant properties
- Their cytotoxicity was evaluated against breast MCF-7 cancer cell line and the human embryonic kidney (Hek293-T) cells